MODELING AND ANALYSIS OF BIMORPH PIEZOELECTROMAGNETIC ENERGY HARVESTER

A thesis submitted in the partial fulfilment

of the requirement for the degree of

Master of Technology

in

Mechanical Engineering

(Specialization: - Machine Design and Analysis)

Submitted by

Satish Balaso Teli

(Roll No: - 213ME1396)

DEPARTMENT OF MECHANICAL ENGINEERING

NATIONAL INSTITUTE OF TECHNOLOGY

ROURKELA- 769008, ODISHA, INDIA

JUNE 2015

MODELING AND ANALYSIS OF BIMORPH PIEZOELECTROMAGNETIC ENERGY HARVESTER

A thesis submitted in the partial fulfilment

of the requirement for the degree of

Master of Technology

in

Mechanical Engineering

(Specialization: - Machine Design and Analysis)

Submitted by

Satish Balaso Teli

(Roll No: - 213ME1396)

Under the supervision of

Prof. J. Srinivas

DEPARTMENT OF MECHANICAL ENGINEERING

NATIONAL INSTITUTE OF TECHNOLOGY

ROURKELA- 769008, ODISHA, INDIA

JUNE 2015

DEPARTMENT OF MECHANICAL ENGINEERING
NATIONAL INSTITUTE OF TECHNOLOGY
ROURKELA- 769008, ODISHA, INDIA

CERTIFICATE

This is to certify that the thesis entitled **"MODELING AND ANALYSIS OF BIMORPH PIEZOELECTROMAGNETIC ENERGY HARVESTER"** submitted by '**Satish Balaso Teli**' to the **National Institute of Technology (NIT), Rourkela** for the award of **Master of Technology** in **Machine Design and Analysis**, is a record of bonafide research work carried out by him in the **Department of Mechanical Engineering**, under the supervision and guidance.

I believe that this thesis fulfils part of the requirements for the award of degree of Master of Technology. The results embodied in the thesis have not been submitted for the award of any other degree elsewhere.

Place: - Rourkela
Date: -

Prof. J. Srinivas
Department of Mechanical Engineering
National Institute of Technology
Rourkela- 769008

ACKNOWLEDGEMENT

My first thanks are to the Almighty God. I am extremely fortunate to be involved in an exciting and challenging research project work on "**Modeling and analysis of bimorph Piezoelectromagnetic Energy Harvester**". I would like to express my greatest gratitude to my supervisor **Prof. J. Srinivas**, for his excellent guidance, valuable suggestions and endless support. He has not only been a wonderful supervisor but also an honest and sincere person. I consider myself extremely lucky to be able to work under guidance of such a dynamic personality.

I would like to express my sincere thanks to Prabhu L, K. V. Varalakshmi, Sk. Jakeer Hussain, Puneet Kumar, R. Reddy and all my classmates for their precious suggestions and encouragement to perform the project work. I am very much thankful to them for giving their valuable time for me.

Finally, I express my sincere gratitude to my parents for their constant encouragement and support at all phases of my life.

SATISH BALASO TELI

ABSTRACT

Piezoelectric energy harvesting is one of the methods of obtaining energy from environment. It is often a cantilever beam with or without tip mass poled with piezoelectric material. The fixed end of cantilever beam is subjected to either base excitation or translation as occurring from an environmental source such as automobile or vibrating engine. The piezoelectric energy harvester generates maximum energy when it is excited at resonance frequency and the little variation below or above the resonance frequency will drastically reduce the power output. In this line, present work studies a broadband nonlinear piezoelectric energy harvester driven by periodic and random oscillations. The simulated response to the base excitation is illustrated in terms of harvested power. By introducing magnetic force, we can broaden the frequency zone so as to capture more energy even the beam do not vibrate close to source frequency. A magnetic tip is included at the free end of the cantilever beam and is excited by two permanent magnets fixed on either sides laterally. The symmetric bimorph cantilever beam piezoelectric energy harvester with magnetic tip is modeled as Single-degree of freedom lumped parameter system. The time domain history and frequency response diagrams for the cantilever displacement, voltage and power at the constant load resistance gives a stability picture as well as the amount of energy harvested. The effect of various parameters of energy harvester system on induced voltage and output power is studied. The distributed parameter model is formulated by using Euler-Bernoulli beam theory and Galerkin's approximation technique. The finite element modeling equations are presented with piezoelectric coupling terms. Novelty in the work include; (i) adding a magnetic force in the system to make it as broadband harvester (ii) validation of approximation solutions with spring-mass modeling.

CONTENTS

LIST OF FIGURES

NOTATION

M_t	Tip mass
M_b	Mass of cantilever beam
m	Mass per unit length of cantilever beam
M_{eq}	Equivalent mass
C_{eq}	Equivalent damping
K_{eq}	Equivalent stiffness
θ_f	Forward coupling term
θ_b	Backward coupling term
Y_s	Young's modulus of substrate
L_s	Length of substrate
Y_p	Young's modulus of piezolayer
L_p	Length of piezolayer
ω_n	Natural frequency
ξ	Damping ratio
μ	Amplitude correction factor
C_p	Clamped capacitance
R_l	Load resistance
f_m	Magnetic force

β	Magnetic flux density
l_m	Length of magnet
B_m	Width of magnet
h_m	Thickness of magnet
τ_0	Permeability of the medium
D_0	Distance between fixed magnet and tip mass
m_1 / m_2	Magnetic dipole moment
C	Strain rate damping coefficient
ϑ	Coefficient of backward coupling term
$\delta(x)$	Dirac delta function
YI	Bending stiffness
e_{31}	Piezoelectric stress constant
h_p	Thickness of piezolayer
h_s	Thickness of substrate
ρ_s	Density of substrate
ρ_p	Density of piezolayer
ϕ_r	Mass normalized Eigen function
λ	Eigen value
χ	Mechanical coupling term
θ_i^e	Elemental coupling term

ψ_i / ψ_j	Hermitian shape functions
E_3	Electric field component
ε_{33}	Permittivity constant
ϖ	Ratio of frequency of base excitation to the natural frequency
w_b	Base excitation
κ	Electrical coupling term

CHAPTER 1

INTRODUCTION

Energy harvesting materials and systems have emerged as a most important research fields and continues to grow at rapid pace. More precisely harvesting the energy from ambient waste for the purpose of running low-powered electronic devices has emerged during the last decade as an enabling technology for wireless applications. An energy harvester have been considered as a green resources and include several advantages such as long lifetime, high power density, low maintenance, simplicity of fabrication, etc. There are several sources available in the environment including sunlight, heat, vibrations, etc. which provoke in the development of various energy harvesters. Of various environmental energy sources vibration energy is found to be available widely and the mechanical vibrations can be converted into electrical energy in a simple way. The goal of the vibration-based energy harvesting technology is to supply power to the microelectronic devices such as sensors and actuators as well as to recharge storage devices like small batteries and capacitors.

1.1 Vibration based energy harvesting

There are main three conversion techniques available by which mechanical vibrations can be converted into electrical form namely electrostatic, electromagnetic and piezoelectric transduction [1, 2]. It can be seen that among all the alternatives available, piezoelectric transduction technique has received comparatively more attention because of high energy density as well as simplicity of conversion. If power density versus voltage output is compared for different transduction techniques, it can be seen that piezoelectric transduction receives the largest area in the plot with power density values comparable to those of lithium-ion batteries, electromagnetic

and thermoelectric generators [3]. Piezoelectric materials generates electric charge when they are subjected to dynamic strain.

The cantilever beam with piezoelectric layers have been frequently used as a piezoelectric energy harvesters due to their high flexible behavior and low natural frequency. When vibration-based cantilever beam energy harvester is excited at its resonance frequency it can generate maximum energy. When external frequency shifts below or above the resonance frequency, the performance of generator drastically reduces. The cantilever beam piezoelectric energy harvester is typically a substructure with one or two piezoceramic layers. If the piezoelectric layer is attached to only one side of the cantilever beam it is called as unimorph piezoelectric energy harvester. If the piezoelectric layer is attached to both the sides of cantilever beam it is called bimorph piezoelectric energy harvester. In the case of bimorph energy harvester; if the piezoceramic layers are oppositely poled in thickness direction then the configuration is known as series connection. Or else if the piezoceramic layers are poled in the same direction, configuration represents parallel connection. Piezoelectric energy harvesting system have wider operating range than other vibration based energy transduction mechanisms especially when dealing with low frequency ambient vibration. A tip-mass can be attached to the free end of the cantilever to reduce the excitation or natural frequency and increase its deflection. A conventional bimorph piezoelectric energy harvester with both the connections is shown in Fig. 1.1 below. A base excitation in the form of both translation (g) and rotation (h) is applied and the induced strain (displacement z) as well as voltage generated (as open circuit and short circuit) in both series and parallel configurations are illustrated. Due to load resistance (R_l), power is generated from the circuit. Just like solar, photovoltaic batteries the generated energy can be stored in small cells or could be used to drive directly the micro vehicle.

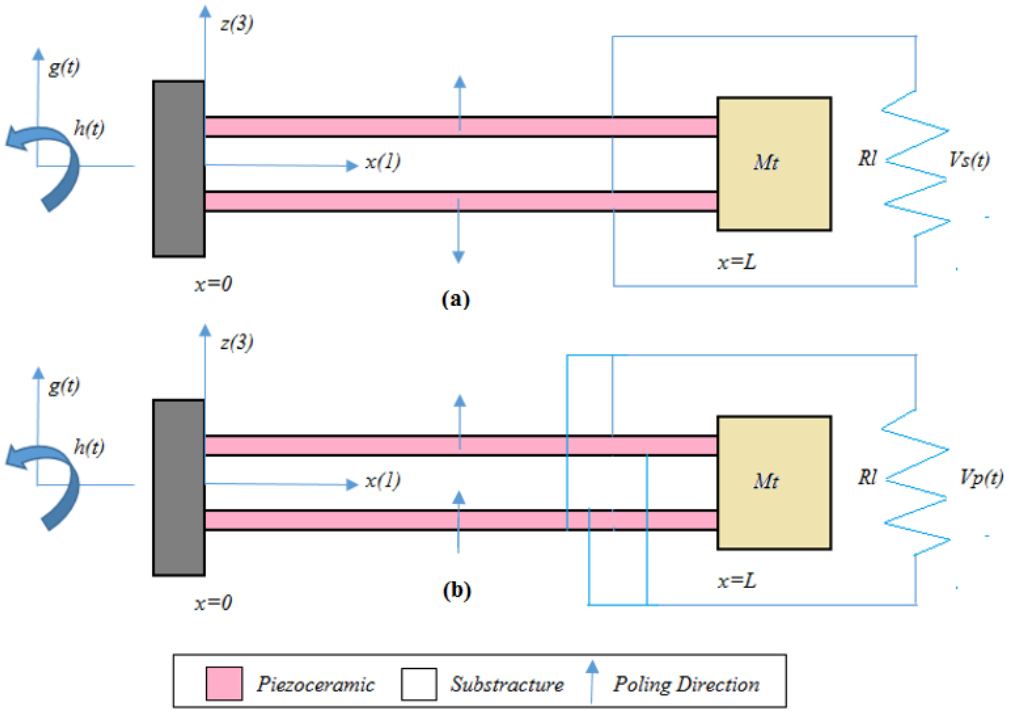

Fig. 1.1 Uniform bimorph piezoelectric energy harvester configurations with (a) Series connection (b) parallel connection of the piezoceramic layers

For harvesting energy with a broadband time dependent frequency characteristics several approaches including oscillator arrays, oscillators with active frequency tuning, etc. were proposed. The dynamic nonlinearities in the harvester systems to enhance the performance can be included as a nonlinear stiffness or as a bistable oscillating system. In the first type of adding nonlinearity the effects of nonlinear stiffness on the energy harvesting ability was considered by several researchers. The bistable energy harvesting systems were implemented with various structures such as bistable magnetic repulsion harvester, bistable electromagnetic attraction harvester as well as buckled cantilever beam harvester. Most of the works focused on first two categories. A novel energy harvester composed of piezoelectric cantilever beam substructure with a magnetic tip mass and two or more external magnets of same polarities, so as to induce a repulsion or attraction force causing a bifurcation behavior which leads to cantilever beam to

behave as a bistable system that can possess two nontrivial stable equilibrium. So this type of systems exhibit a good broadband harvesting performance and produces a large voltage.

1.2 Literature review

Energy harvesting from environmental sources especially mechanical vibrations have paid a lot of attention in the past five to ten years. In this section, various research works previously done are arranged in systematic manner.

1.2.1 Single and Multi-DOF Piezoelectric Energy Harvester

Single degree of freedom piezoelectric energy harvesters are only efficient near sole resonance limits. Tang and Yang [4] presented an article regarding a novel multi degree of freedom piezoelectric energy harvesting model. By analyzing the two degree of freedom energy harvester model they considered its two configurations for characterization. Finally the model is generalized to n-degree of freedom system and its mathematical solution is derived which can be used as a reference for parametric study and design of multi degree of freedom energy harvesters. The article is concluded by developing equivalent circuit model for multi-degree of freedom piezoelectric energy harvesters.

Usually conventional energy harvester is excited at its first resonance mode and all the characteristics are studied at first mode only but Wu et al. [5] considered first two vibration modes. The presented design is giving significant power output and is functional in practical vibrational circumstances.

Different types of excitations can be provided to the linear single-degree of freedom piezoelectric energy harvester. The ambient vibration energy is random in nature hence Joo and Sapsis [6] worked on applying different type of excitations to the harvesters so as to develop the performance criteria. They summarized their work by concluding that whatever may be the

excitation provided to the linear energy harvester, its output can't be increased above the optimal performance of the linear harvester and it is less than nonlinear design.

Most of the researchers have contributed to get the experimental results and practical applications of already developed conventional piezoelectric energy harvesters. Khalatkar et al. [7] developed an energy harvester which can be excited by engine vibrations and harvest at least micro level electrical energy.

1.2.2 Lumped Parameter Models

Most of the early research is based on analyzing the piezoelectric energy harvester as a lumped parameter model in which the equations of motion are derived by using D'Alembert's principle or by applying Newton's second law in mechanical domain and Kirchhoff's law in electrical domain. Most of the researchers worked on analyzing the optimal AC power output but Shu and Lien [8] investigated the optimal AC-DC power generation for rectified piezoelectric micro generator. They analyzed energy harvester as lumped parameter model and finally concluded their research by providing several design guidelines for real time applications of energy harvester.

It is well known fact that when resonant frequency of energy harvester matches with the ambient vibration one can get maximum energy output. Generated power exponentially reduces ever for smaller difference between these two frequencies. Zhu et al. [9] worked on different strategies of reducing the resonant frequency of excitation of energy harvester and summarized their work by providing advantages as well as disadvantages of each strategy.

The position of tip mass along the length of cantilever beam also have a considerable effect on the power harvested from energy harvester. Piezoelectric energy harvester has a limited power

output and hence device performance should be enhanced to get the optimum power output. Ali and Ibrahim [10] worked on these issues along with some experiments.

There two main limitations of conventional energy harvesters. Firstly, energy harvesting ability only along one direction. Secondly, its ability to harvest energy only in the narrow band of frequency. But in real case ambient vibrations are spread along several orientations which can reduces the power output. To overcome all these limitations many researchers are working on broadband, multi-directional vibrational energy harvesting. Ando et al. [11] presented bi-directional, broadband piezoelectromagnetic energy harvester. They added nonlinearity by providing permanent magnets and two cantilever beams are kept perpendicular to each other.

Generally piezoelectric energy harvesters are excited under sinusoidal base excitation but it is not the practical case because environmental excitations are random in nature. Jiang and Chen [12] proposed technique to determine approximately the voltage output of a nonlinear energy harvester excited under Gaussian white noise excitations. Equivalent linear system is derived from minimizing the mean squared of the error. The linear equivalent coefficients are presented by the method of normal truncation. The exact solution of equivalent linear system is obtained and the effectiveness of the method is demonstrated by numerical solutions.

1.2.3 Distributed Parameter Models

Along with lumped parameter modelling, the research is also focused on considering cantilever beam along piezoceramic layer as single or multi-degree of freedom distributed parameter model which can be solved by using Euler-Bernoulli or Thimoshenko beam theory. Erturk and Inman [13] gave an exact solution of energy harvester for unimorph harmonic base excitation case and investigated its behavior under short circuit and open circuit conditions. Erturk and Inman also reviewed [14] most general case of energy harvester that is cantilever beam. It is

modeled by using Euler-Bernoulli beam theory and results are compared with single degree of freedom energy harvester. It is concluded that single degree of freedom piezoelectric energy harvester gives highly inaccurate results and hence Erturk and Inman introduced correction factor.

Energy harvesting along the wide range of excitation frequency is called as Broadband energy harvesting and it is recently focused area in the field of piezoelectric energy harvesting. Adam [15] designed a real time energy harvester which can harvest energy by using car vibrations white driving. The design is modified by adding the non-linearity such as applying magnetic tip mass at its free end for broadband energy harvesting purpose.

When cantilever beam is excited near twice of its natural frequency it is termed as principal parametric excitation. A distributed parameter reduced order model is developed by Abdelkefi et al. [16] by using Euler-Lagrange principle and Gauss Law which is excited under parametric excitation. The model is discretized under Galerkin's principle and the effect of different nonlinear piezoelectric coefficients on the power harvested are discussed.

Many researchers have attempted different shaped piezoelectric energy harvesters to get the optimum power output. Diyana et al. [17] presented comb shaped piezoelectric energy harvester and is solved using Euler-Bernoulli beam theory. Xiong and Oyadiji [18] contributed towards finding the optimum beam shape for cantilevered beam piezoelectric energy harvester and investigated that both convergent and divergent energy harvesters with tip mass attached can generate more energy. They also studied the effect various geometric parameters on energy harvesting capability.

In the real time application of piezoelectric energy harvester excitation frequency range is below 1000 Hz. Proof mass at the end reduces the excitation frequency of energy harvester hence it should be chosen appropriately based on the ambient frequency range in which generator is

going to be mounted. Fakhzan and Muthalif [19] presented an energy harvester for multi-mode vibration which is modeled by considering Euler-Bernoulli beam theory. They also presented the importance of position proof mass over the cantilever beam.

Fourier Transform Green's function is an alternative technique to solve distributed parameter energy harvester. Danesh-Yazdi et al. [20] developed the solution of piezoelectric energy harvester beam under Green's function method.

The main focus of Muthalif and Nordin [21] was to study the optimal beam shape of piezoelectric energy harvester for both single harmonic and broadband vibration. Mathematical derivations for unimorph piezoelectric energy harvester are presented. They also studied the effect of varying the length and shape of the beam on the output power. Triangular shape exhibits the highest voltage generated within the desired frequency range.

1.2.4 Finite element Analysis of Piezoelectric Energy Harvester

Finite element analysis is the effective tool for validation of all the types of energy harvesters discussed above and hence so many researchers worked in this area. Marqui formulated [22] coupled FE plate model for getting the output voltage and power of energy harvester. The results obtained from FE model are then compared with analytical solution of unimorph cantilever beam piezoelectric energy harvester.

Wang [23] studied the effectiveness of Euler-Bernoulli and Thimoshenko beam theory for bimorph piezoelectric energy harvester. Euler-Bernoulli theory is applicable for slender piezoelectric beams whereas Thimoshenko theory should be applied for short beams.

Eziwarman [24] presented two numerical techniques for finite element analysis of energy harvester. Euler-Bernoulli beam assumption is used for formulation of fundamental beam equations and electromechanical discretization is used to model the piezoelectric structure along

with extended Hamiltonian principle. Again orthonormalised electromechanical FE response technique is used to get accurate frequency domain results.

Lead based materials have been banned from last five years in many countries hence PZT can't be directly used for energy harvesting application hence an alternative piezoceramic material is to be found out. Material issues in piezoelectricity is another huge research area and many researchers are working in this field. Kumar et al. [25] worked on a performance of various piezoelectric materials piezoelectric energy harvesting application. The finite element method is used to model piezolaminated unimorph cantilever structure. First order shear deformation theory is implemented in finite element simulations. Genetic Algorithm is used to optimize the mechanical parameters for maximum power density and power output.

Most of the early research regarding FE analysis of energy harvester was concentrated on homogeneous beam structures. Recently some of the functionally graded piezoelectric materials are developed due to brittle behavior of conventional piezoelectric materials. Amini et al. [26] worked on finite element analysis of functionally graded piezoelectric energy harvesters for unimorph as well as bimorph case.

1.2.5 Piezoelectromagnetic Energy Harvesters

There are so many researchers worked on conventional piezoelectric energy harvesters however adding nonlinearity in the base excitation is recently focused area. Nonlinearity in the piezoelectromagnetic energy harvester can be incorporated by introducing softening and hardening response. An energy harvester presented by Stanton et al. [27] is bidirectional with both softening and hardening response within quadratic potential field. It is experimentally validated that nonlinear energy harvester will adopt broadband energy harvesting as compared to equivalent linear energy harvester.

Zhou et al. [28] investigated vertically aligned magnetically coupled nonlinear piezoelectric energy harvester. By altering the angular orientation of its external magnets enhanced broadband frequency response can be achieved and low frequency response is achieved by changing the magnetic orientation. Finally the work is experimentally explored for validation purpose.

Ibrahim et al. [29] worked on mathematical modelling and simulation of lumped parameter piezoelectric energy harvester with tip mass attached at the free end of the cantilever beam and fixed magnet at only one side of the beam. The proposed piezoelectromagnetic harvester is compared with conventional cantilever beam harvester with tip mass.

Fan et al. [30] developed two magnetically coupled compact piezoelectric cantilever beams with orthogonal directions of deflection for broadband energy harvesting and results are validated with experiment. The proposed energy harvester shows improved performance in voltage output as compared to linear energy harvesters.

The energy harvester presented by Kim and Seak [31] uses the magnetic attraction effect between the soft magnetic tip of the cantilever beam and the two externally fixed permanent magnets arranged in series. Finally nonlinear dynamic and energetic characteristics of the multi-stable energy harvester were examined by utilizing the bifurcation analysis and a series of numerical simulations.

Jung et al. [32] modelled cantilever beam nonlinear dynamic piezoelectric energy harvester with tip magnet and two external rotatable external magnets fixed in free space using modified Hamilton's principle. Mathematical modelling of cantilever beam and magnetic force expression is derived using Euler-Bernoulli beam theory and magnetic current model respectively and results are validated with the experiment.

Shafer and Garcia [33] presented upper limits of input acceleration and output power for a piezoelectric harvester device.

Litak et al. [34] described the piezoelectromagnetic energy harvester with stationary Gaussian White noise.

1.3 Scope and Objective of the present work

Based on the above highlighted literatures, it is found that broadband energy harvesting is the recently focused area. To the conventional cantilever beam energy harvester, magnetic tip mass can be added and cantilever beam can be excited in additional magnetic field along with base excitation. In this regard, it is planned to develop a bistable piezoelectromagnetic energy harvesting system which can exhibit a good broadband harvesting performance and produces large voltage. Given below are the objectives of present work:-

i. Mathematical modelling and simulation of lumped parameter bimorph cantilever beam piezoelectric energy harvester with magnetic tip and additional magnetic field.
ii. To formulate and simulate distributed parameter bimorph piezoelectric energy harvester with tip magnet and additional magnetic force to the base excitation.
iii. To study the various parameters which influence induced voltage and power.
iv. Finite element analysis of piezoelectric energy harvester.

The present thesis is organized as follows:-

Chapter 2 presents the mathematical modeling of lumped parameter as well as distributed parameter model bimorph piezoelectric energy harvester with tip mass and additional magnetic field to the base excitation. The finite element analysis approach is also presented at the end.

In Chapter 3, the results and discussion of the present work is arranged in systematic manner.

Chapter 4 contains the conclusion of the present work along with the future scope.

CHAPTER 2

MATHEMATICAL MODELING

This chapter includes mathematical modeling of proposed piezoelectric energy harvester. The finite element modeling is also added at the end.

2.1 Lumped parameter modeling

A typical schematic of spring-mass-damper system of lumped parameter piezoelectric energy harvester is shown in Fig. 2.1, with the base excitation $x_0(t)$. The system can be modeled as a single degree of freedom system and the equations of motion [29] for piezoelectric energy harvester are derived by applying Newton's law in the mechanical domain as well as Kirchhoff's law in electrical domain.

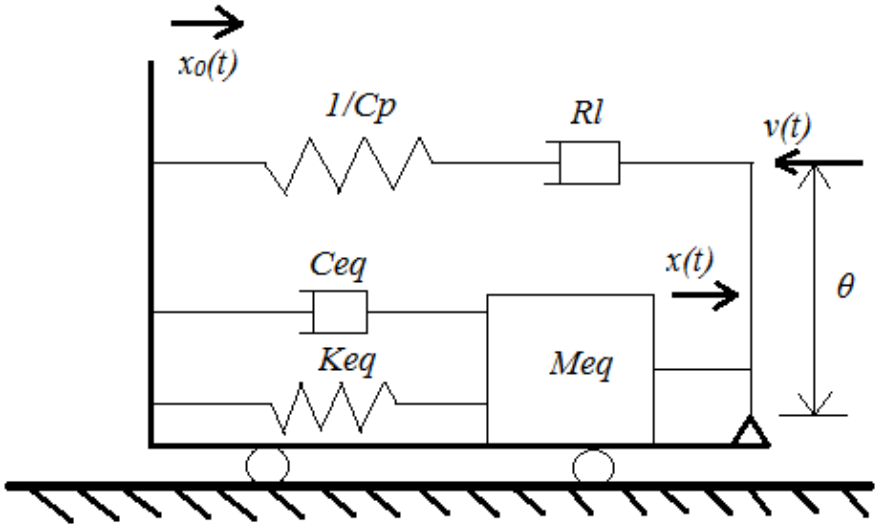

Fig. 2.1 Single-DOF piezoelectric energy harvester

$$M_{eq} \times \ddot{x}(t) + C_{eq} \times \dot{x}(t) + K_{eq} \times x(t) + \theta_b \times v(t) + f_m = -\mu \times M_{eq} \times \ddot{x}_0(t) \tag{2.1}$$

$$I(t)+C_p\times\dot{v}(t)-\theta_f\times\dot{x}(t)=0 \tag{2.2}$$

Equations (2.1) and (2.2) represents both mechanical and electrical domain of the piezoelectric energy harvester respectively. $x(t)$ is the relative displacement of the tip mass M_t and M_{eq}, C_{eq} and K_{eq} equivalent mass, damping and stiffness of the piezoelectric energy harvester respectively. $v(t)$ is the induced voltage in the harvester due to mechanical vibration. θ_f and θ_b are forward and backward electromechanical effects respectively. Equivalent mass, damping and stiffness can be calculated by using the equations below

$$M_{eq}=\frac{33}{140}m+M_t \tag{2.3}$$

$$K_{eq}=K_{substrate}+K_{patch}=\left(\frac{3Y_sI_s}{L_s^3}\right)_{substrate}+\left(\frac{3Y_pI_p}{L_p^3}\right)_{patch} \tag{2.4}$$

$$C_{eq}=2\xi M_{eq}\omega_n \tag{2.5}$$

Here, ξ is the damping ratio. The natural frequency of the energy harvester is calculated by using the fundamental relation as

$$\omega_n=\sqrt{\frac{K_{eq}}{M_{eq}}} \tag{2.6}$$

The term μ is the amplitude correction factor for improving the lumped parameter model and it is calculated by using the equation [29] as

$$\mu = \frac{\left(M_t / M_b\right)^2 + 0.60 \times \left(M_t / M_b\right) + 0.09}{\left(M_t / M_b\right)^2 + 0.46 \times \left(M_t / M_b\right) + 0.06} \tag{2.7}$$

Where, $\left(M_t / M_b\right)$ is the ratio of tip mass to distributed mass of the beam; $I(t)$ and $v(t)$ are induced current and voltage of the piezoelectric energy harvester due to vibration of the beam; C_p is the clamped capacitance of the piezoelectric transducer. From Ohm's law,

$$v(t) = I(t) \times R_l \tag{2.8}$$

Here, R_l is the load resistance of the piezoelectric circuit. Putting the value of $I(t)$ in the eq. (2.2), one can get following equation

$$v(t)/R_l + C_p \times \dot{v}(t) - \theta_f \times \dot{x}(t) = 0 \tag{2.9}$$

The magnetic force term (f_m) to the right hand side of the eq. (2.1) is formulated on the basis of following assumptions

I. There is magnetic dipole coupling between the magnets.

II. The magnetic dipoles are always perpendicularly aligned when the piezoelectric beam vibrates.

$$f_m = \left[\frac{\beta^2 A^2 \left(l_m + r_m\right)^2}{\pi \tau_0 l_m^2}\right]\left[\frac{1}{D_0^2} + \frac{1}{\left(D_0 + 2l_m\right)^2} - \frac{2}{\left(D_0 + l_m\right)^2}\right] \tag{2.10}$$

When $l_m \ll D_0$ the approximation of magnetic force is

$$f_m = \frac{-3\tau_0 m_1 m_2}{2\pi\left[D_0\right]^4} \tag{2.11}$$

Where, τ_0 is the permeability of the medium (i.e. air), D_0 is the distance between the two magnets which is identical to the both sides. β is the magnetic flux density. The magnetic dipole moments m_1 and m_2 of the identical magnets are formulated by the following equation

$$m_1 / m_2 = \frac{2\beta V}{\tau_0} \tag{2.12}$$

Where, volume (V) of each magnet depends upon the geometric parameters of the magnet. The fundamental law of magnetism states the following two cases

I. For the two attractive magnets, $m_1 = -m_2$

II. For the two repulsive magnets, $m_1 = m_2$

The proposed energy harvesting system contains fixed magnets at both the sides of tip magnet. Hence, the total magnetic force is

$$f_m = \frac{-3\tau_0 m_1 m_2}{\pi\left[D_0\right]^4} \tag{2.13}$$

If the tip displacement of piezoelectric energy harvesting system is added to the magnetic force then magnetic force expression can be written as

$$f_m(t) = \frac{-3\tau_0 \times m_1 \times m_2}{\pi\left[x(t) + D_0\right]^4} \tag{2.14}$$

Now, the coupled electromechanical governing equation of motion for the presented piezoelectric energy harvester can be represented by following expression

$$M_{eq}\times\ddot{x}(t)+C_{eq}\times\dot{x}(t)+K_{eq}\times x(t)+\theta_b\times v(t)-\frac{3\tau_0\times m_1\times m_2}{\pi\left[x(t)+D_0\right]^4}=-\mu\times M_{eq}\times\ddot{x}_0(t) \tag{2.15}$$

$$v(t)\Big/R_l+C_p\times\dot{v}(t)-\theta_f\times\dot{x}(t)=0 \tag{2.16}$$

The above two equations are electromechanically coupled as both contain displacement and voltage terms. Hence, these second order differential equations should be converted into multiple first order form by using state variables for solving them simultaneously. The corresponding state variables are shown in eq. (2.17) below.

$$z_1(t)=x(t),\ z_2(t)=\dot{x}(t)\text{ and }\ z_3(t)=v(t) \tag{2.17}$$

$$\dot{z}_1(t)=z_2(t) \tag{2.18}$$

$$\dot{z}_2(t)=-\frac{C_{eq}}{M_{eq}}z_2(t)-\frac{K_{eq}}{M_{eq}}z_1(t)-\frac{\theta_b}{M_{eq}}z_3(t)+\frac{3\tau_0\times m_1\times m_2}{\pi\times M_{eq}\left[z_1(t)+D_0\right]^4}-\mu\times\ddot{x}_0(t) \tag{2.19}$$

$$\dot{z}_3(t)=\frac{\theta_f}{C_p}z_2(t)-\frac{1}{R_l\times C_p}z_3(t) \tag{2.20}$$

The corresponding first order equations (2.18), (2.19) and (2.20) are solved by using Runge-Kutta method in Matlab software to get the tip mass displacement and equivalent voltage responses. To find out the maximum tip mass amplitude and corresponding induced voltage following equations [8] are to be considered.

$$x_{\max} = \frac{M_{eq} \times \varpi^2 \times U\left(\frac{1}{R_l} + j \times C_p \times \varpi\right)}{\left\{\left(K_{eq} - M_{eq}\varpi^2\right) + j \times C_{eq} \times \varpi\right\}\left(\frac{1}{R_l} + j \times C_p \times \varpi\right) + j \times \varpi \times \theta^2} \tag{2.21}$$

And

$$V_{\max} = \frac{j \times U \times \theta \times \varpi^3}{\left\{\left(K_{eq} - M_{eq}\varpi^2\right) + j \times C_{eq} \times \varpi\right\}\left(\frac{1}{R_l} + j \times C_p \times \varpi\right) + j \times \varpi \times \theta^2} \tag{2.22}$$

Here, $\varpi = \frac{\omega}{\omega_n}$ is the ratio of frequency of base excitation to the natural frequency of the harvester.

The term U is the total excitation provided to the harvester.

2.2 Distributed parameter modeling

A novel energy harvester composed of piezoelectric cantilever beam with a tip mass and external magnets of same polarities, so as to induce a repulsion or attraction force causing a bifurcation behavior which leads to cantilever beam to become a bistable system that includes two nontrivial stable equilibrium. So this type of systems exhibit a good broadband harvesting performance and produces large voltage. In this section, the symmetric bimorph cantilever beam configuration is modelled as a uniform composite beam based on Euler-Bernoulli beam theory. The Fig. 2.2 represents the bimorph piezoelectric energy harvester with tip mass at the free end and additional magnetic field to the base excitation.

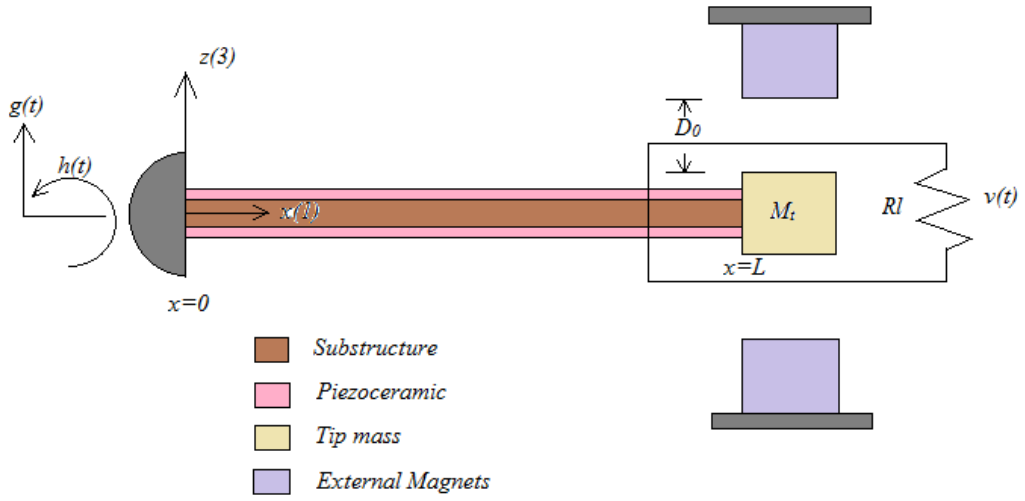

Fig. 2.2 Energy harvester with tip mass and fixed external magnets

The base excitation of the cantilever beam is represented by translational displacement $g(t)$ in the transverse direction with superimposed small rotational displacement $h(t)$. Hence, the effective base displacement can be written as

$$w_b(x,t) = g(t) + x \times h(t) \tag{2.23}$$

The coupled mechanical equation [32] motion can be obtained for series connection as

$$YI\frac{\partial^4 w(x,t)}{\partial x^4} - \vartheta \times v(t)\left[\frac{d\delta(x)}{dx} - \frac{d\delta(x-L)}{dx}\right] + CI\frac{\partial^5 w(x,t)}{\partial x^4 \times \partial t} + m\frac{\partial^2 w(x,t)}{\partial t^2} = -m\frac{\partial^2 w_b(x,t)}{\partial t^2} + f_m\frac{\partial^2 w(x,t)}{\partial x^2} \tag{2.24}$$

Where $w(x,t)$ is the transverse displacement of the beam relative to its base at position *x* and time *t*, $v(t)$ is the voltage across electrodes of piezoceramic layers, m is the mass per unit length of the beam, M_t is the tip mass, C is the strain-rate damping coefficient, ϑ is the coefficient of backward

coupling term, f_m is the *x*-directional magnetic force and $\delta(x)$ is the Dirac delta function. The partial differential eq. (2.24) is solved with following assumptions:

(1) External magnets are fixed in space.

(2) Only transverse magnetic force is considered for boundary conditions.

The corresponding boundary conditions are

$$\text{At } x=0;\ w=0 \text{ and } \frac{\partial w}{\partial x}=0 \tag{2.25}$$

At $x=L$;

$$YI\frac{\partial^2 w(x,t)}{\partial x^2}+CI\frac{\partial^3 w(x,t)}{\partial x^2\times\partial t}=0 \tag{2.26}$$

$$-YI\frac{\partial^2 w(x,t)}{\partial x^2}-CI\frac{\partial^4 w(x,t)}{\partial x^3\times\partial t}+f_m\frac{\partial w(x,t)}{\partial x}=M_t\left(\frac{\partial^2 w(x,t)}{\partial t^2}+\frac{\partial^2 w_b(x,t)}{\partial t^2}\right) \tag{2.27}$$

The coefficient of backward coupling (ϑ), bending stiffness term (YI) and mass per unit length (m) of the composite cross-section of the piezoceramic are given [34] by

$$\vartheta=\frac{e_{31}}{2h_p}\left[\left(h_p+\frac{h_s}{2}\right)^2-\frac{h_s^2}{4}\right] \tag{2.28}$$

$$YI=\frac{2B}{3}\left\{Y_s\frac{h_s^3}{8}+Y_p\left[\left(h_p+\frac{h_s}{2}\right)^3-\frac{h_s^3}{8}\right]\right\} \tag{2.29}$$

$$m=B\left(\rho_s h_s+2\rho_p h_p\right) \tag{2.30}$$

The magnetic force expression in the eq. (2.24) is same as that of lumped parameter case as previously described hence magnetic force expression for proposed piezoelectric energy harvesting system is given by

$$f_m(t) = \frac{-3\tau_0 \times m_1 \times m_2}{\pi\left[x(t) + D_0\right]^4} \tag{2.31}$$

Based on proportional damping assumption, the vibration response relative to the base of the bimorph cantilever can be represented as a convergent series of the Eigen functions as

$$w(x,t) = \phi_r(x) \times \eta(t) \tag{2.32}$$

Where $\phi_r(x)$ is the mass-normalized Eigen function for r^{th} vibration mode and $\eta(t)$ is modal mechanical coordinate expression of the series connection. Considering $r = 1$, $\phi(x)$ can be calculated as

$$\phi(x) = A\left[\cos\frac{\lambda}{L}x - \cosh\frac{\lambda}{L}x + \varsigma\left(\sin\frac{\lambda}{L}x - \sinh\frac{\lambda}{L}x\right)\right] \tag{2.33}$$

Where ς is obtained from

$$\varsigma = \frac{\sin\lambda - \sinh\lambda + \left(\lambda\frac{M_t}{mL}\right)(\cos\lambda - \cosh\lambda)}{\cos\lambda + \cosh\lambda - \left(\lambda\frac{M_t}{mL}\right)(\sin\lambda - \sinh\lambda)} \tag{2.34}$$

ω is the undamped natural frequency of first vibration mode. It is given by

$$\omega = \lambda^2\sqrt{\frac{YI}{mL^4}} \tag{2.35}$$

The eigenvalues of the system are obtained from the equation [34] given below

$$1+\cos\lambda\times\cosh\lambda+\left(\lambda\frac{M_t}{mL}\right)\left(\cos\lambda\times\cosh\lambda-\sin\lambda\times\sinh\lambda\right)-\left(\frac{\lambda^3 I_t}{mL^3}\right)\left(\cosh\lambda\times\sin\lambda+\sinh\lambda\times\cos\lambda\right)$$
$$+\left(\frac{\lambda^4 M_t I_t}{m^2 L^4}\right)\left(1-\cos\lambda\times\cosh\lambda\right)=0 \tag{2.36}$$

After substituting eq. (2.32) into eq. (2.24) and applying boundary conditions for undamped problem, the mechanical equation of motion can be obtained as

$$\frac{d^2\eta(t)}{dt^2}+2\xi\times\omega\frac{d\eta(t)}{dt}+\omega^2\times\eta(t)-\chi\times v(t)=f_r(t)+f_m(t) \tag{2.37}$$

Where the modal mechanical coupling term is

$$\chi=\frac{\vartheta\times d\phi(x)}{dx} \tag{2.38}$$

The modal mechanical forcing function [34] and magnetic force due to tip magnet and two external fixed magnets can be expressed as

$$f_r(t)=-m\left(\frac{d^2g(t)}{dt^2}\int_0^L\phi(x)dx+\frac{d^2h(t)}{dt^2}\int_0^L x\times\phi(x)dx\right)-M_t\times\phi(L)\left(\frac{d^2g(t)}{dt^2}+L\times\frac{d^2h(t)}{dt^2}\right) \tag{2.39}$$

$$f_m(t)=\frac{-3\tau_0\times m_1\times m_2}{\pi\left[\phi(x)\times\eta(t)+D_0\right]^4} \tag{2.40}$$

Here, ξ is the equivalent modal mechanical damping ratio that includes both strain rate damping and air damping. The piezoelectric layers of the bimorph configuration shown in Fig. 2.2 are

connected in series. Kirchoff's laws can be applied to obtain the coupled electrical circuit equation as given below

$$\frac{C_p}{2}\frac{dv(t)}{dt}+\frac{v(t)}{R_l}-\kappa\frac{d\eta(t)}{dt}=0 \tag{2.41}$$

$$C_p=\frac{\varepsilon_{33}\times BL}{h_p} \tag{2.42}$$

$$\kappa=\frac{Y_p\times\left(h_p+h_s\right)}{2}\frac{d\phi(x)}{dt} \tag{2.43}$$

Hence, the eq. (2.41) is the electrical circuit equation of the bimorph cantilever for the series connection of the piezoelectric layers. The eq. (2.37) and (2.41) are second order coupled equations with time dependent displacement parameter and voltage parameter. For the simulation purpose one can convert them into multiple first order form by using state variables presented in eq. (2.44).

$$z_1(t)=\eta(t);\ z_2(t)=\frac{d\eta(t)}{dt}=\dot{\eta}(t)\text{ and }\ z_3(t)=v(t) \tag{2.44}$$

$$\dot{z}_1(t)=z_2(t) \tag{2.45}$$

$$\dot{z}_2(t)=\left[f(t)+f_m(t)\right]-2\xi\times\omega\times z_2(t)-\omega^2\times z_1(t)+\chi\times z_3(t) \tag{2.46}$$

$$\dot{z}_3(t)=\frac{-2}{R_l\times C_p}\times z_3(t)-\frac{2\kappa}{C_p}\times z_3(t) \tag{2.47}$$

These equations can be simulated in Matlab for getting time dependent parameter and voltage parameter. Finally by using the mathematical equations stated previously transverse displacement of the beam and corresponding voltage can be calculated.

2.3 Finite Element Modeling

The schematic drawing of bimorph piezoelectric energy harvester with tip mass is shown in Fig. 2.3 below.

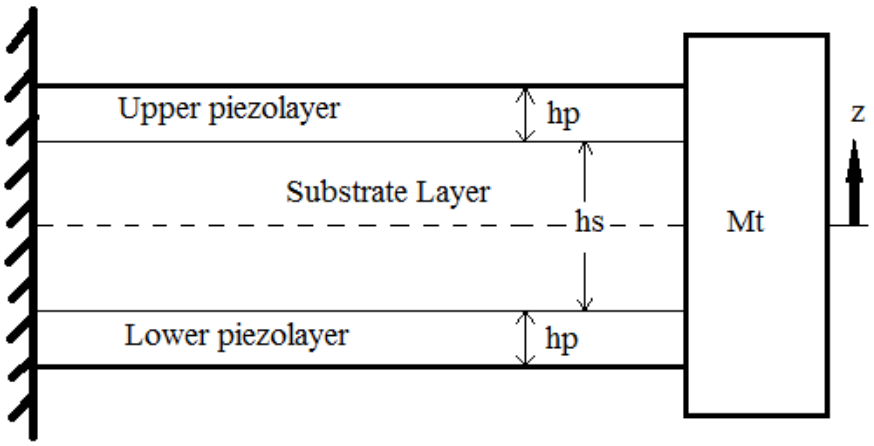

Fig. 2.3 Bimorph piezoelectric energy harvester with tip mass

In the above figure, z is the coordinate through the thickness direction of energy harvester and its origin is assumed to be located at the middle line of harvester as shown in above figure. Here, L and B are the total length and width of the cantilever beam shown above. M_t is the tip mass attached at the free end. For the purpose of finite element modeling, the above cantilever beam is divided into discrete number of elements and each elemental length is $l = L/n$ (n is the number of elements). The Fig. 2.4 below represents local degree of freedom for one of the discretized beam element.

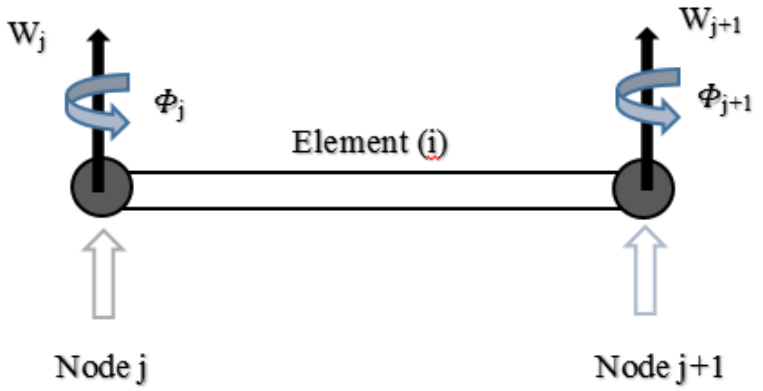

Fig. 2.4 Local degree of freedom for beam element

The elements and nodes are represented by symbol i and j respectively. In the above figure, an element i is represented by its two equivalent nodes j and j+1. At each node two degrees of freedom are considered. W_j is the transverse degree of freedom and Φj is the equivalent rotational degree of freedom at each node. The finite element model presented here can be generalized for infinite number of elements. By using the extended Hamilton's principle the following system of ordinary differential equations [26] is obtained for each element.

$$M_{ij}^{e} \times \ddot{\Delta}_{j}^{e} + C_{ij}^{e} \times \dot{\Delta}_{j}^{e} + K_{ij}^{e} \times \Delta_{j}^{e} - \theta_{i}^{e} \times v(t) = F_{i}^{e} \tag{2.48}$$

$$C_{p} \times \frac{dv}{dt} + \frac{v}{R_{l}} + \left(\theta_{i}^{e}\right)^{T} \times \dot{\Delta}_{i}^{e} = 0 \tag{2.49}$$

Where, R_l is the load resistance value and v is the induced voltage. M^e, K^e and C^e are elemental mass, stiffness and damping matrices respectively. For the purpose of simplicity the damping term can be ignored. F^e is equivalent force vector and Δ^e is described as

$$\Delta = \begin{Bmatrix} W_j & \phi_j & W_{j+1} & \phi_{j+1} \end{Bmatrix}^{T} \tag{2.50}$$

The equivalent mass matrix (M_{ij}^{e}) and stiffness matrix (K_{ij}^{e}) for an element are defined as follows

$$M_{ij}^{e} = \int_{0}^{L} \left(D_p \frac{d\psi_i}{dx} \frac{d\psi_j}{dx} \right) dx \tag{2.51}$$

$$K_{ij}^{e} = \int_{0}^{L} D_p \frac{d^2\psi_i}{dx^2} \frac{d^2\psi_j}{dx^2} dx \tag{2.52}$$

Where ψ_i and ψ_j are Hermitian Shape functions. The term D_p in the above equations can be formulated as

$$D_p = \rho \times \frac{h_p^3}{3} \tag{2.53}$$

The term ρ is equivalent density of substrate and piezolayer. By using the Hermitian shape functions, elemental mass matrix and stiffness matrix of the proposed energy harvester can be calculated as

$$M_{ij}^{e} = \frac{(\rho A) l}{420} \begin{bmatrix} 156 & 22l & 54 & -13l \\ 22l & 4l^2 & 13l & -3l^2 \\ 54 & 13l & 156 & -22l \\ -13l & -3l^2 & -22l & 4l^2 \end{bmatrix} \tag{2.54}$$

Here, ρA is the mass per unit length of each element.

$$K_{ij}^{e} = \frac{(YI)}{l^3} \begin{bmatrix} 12 & 6l & -12 & 6l \\ 6l & 4l^2 & -6l & 2l^2 \\ -12 & -6l & 12 & -6l \\ 6l & 2l^2 & -6l & 4l^2 \end{bmatrix} \tag{2.55}$$

Here, *YI* is the flexural rigidity of each element. In the above eq. (2.48) and (2.49), the coupling term θ_i^e and clamped capacitance C_p are defined as

$$\theta_i^e = \frac{1}{v}\begin{Bmatrix} 0 & -B_e E_3 & 0 & B_e E_3 \end{Bmatrix} \tag{2.56}$$

$$C_p = \frac{A_\varepsilon L}{4h_p^2} \qquad \text{(For series configuration)} \tag{2.57}$$

Where the term E_3 is electric field component in the poling direction and its value for the bimorph series connection is equal to $E_3 = \frac{-v}{2h_p}$. For parallel connection, the electric fields in top layer and bottom layer are $E_3 = \frac{-v}{h_p}$ and $E_3 = \frac{v}{h_p}$. The terms B_e and A_ε in the above equation are calculated as

$$B_e = \int B \times e_{31} \times z \cdot dz \tag{2.58}$$

$$A_\varepsilon = \int B \times \varepsilon_{33}(z)\, dz \tag{2.59}$$

The above two equations should integrated over piezoelectric thickness only. Here e_{31} is piezoelectric stress constant and ε_{33} is the permittivity constant. The base of the proposed piezoelectric energy harvester vibrates in the transverse direction. Therefore, the equivalent forcing term [26] can be given by

$$F_i^e = F_{0i} \times \frac{d^2 w_b}{dt^2} \tag{2.60}$$

Where,

$$F_{0i} = \int_0^L \left(m + M_t \delta\left(x - L\right)\right)\psi_i dx \tag{2.61}$$

Where, m is the mass per unit length of the cantilever beam, M_t is the tip mass attached at the free end of the cantilever beam and $\frac{d^2 w_b}{dt^2}$ is the base acceleration provided. All the above equations can be added to eq. (2.48) and eq. (2.49) so that global form of coupled mechanical and coupled electrical equations can be formulated as

$$[M]^G \times [\ddot{\Delta}] + [K]^G \times [\Delta] - [\theta]^G \times v(t) = [F]^G \tag{2.62}$$

$$C_p \times \frac{dv}{dt} + \frac{v}{R_l} + \left([\theta]^G\right)^T \times [\dot{\Delta}]^G = 0 \tag{2.63}$$

Here $[M]^G$, $[K]^G$ and $[F]^G$ are global mass, stiffness and force vector. $[\theta]^G$ is the global coupling term. Finally above equations can be analytically simulated in Matlab software and can be solved by using Runge-Kutta solver technique. The transverse displacement and equivalent induced voltage can be calculated.

2.4 Solution techniques

There are different solution techniques which can be adopted for the solution of partial differential equations. The distributed parameter model can be solved by using Galerkin's method.

2.4.1 Galerkin's approximate method

In this method the relative displacement is considered as the function of eigenfunction $\phi(x)$ and modal mechanical coordinate $\eta(t)$. The mechanical equation of motion 2.24 is partial differential equation. After substituting the eq. (2.32) into eq. (2.24) one can get

$$YI \times \phi^{iv}(x) \times \eta(t) - \vartheta \times v(t) \times \left[\frac{d\delta(x)}{dx} - \frac{d\delta(x-L)}{dx} \right] + CI \times \phi^{iv}(x) \times \dot{\eta}(t) + m \times \phi(x) \times \ddot{\eta}(t) = -m \times \frac{d^2 w_b(x,t)}{dt^2} + f_m \times \phi^{ii}(x) \times \eta(t) \tag{2.64}$$

The fourth order derivative of eigenfunction is

$$\phi^{iv}(x) = \left(\frac{\lambda}{L} \right)^4 \times \phi(x) \tag{2.65}$$

Substituting eq. (2.65) in eq. (2.64), the mechanical equation reduces to

$$YI \times \left(\frac{\lambda}{L} \right)^4 \times \phi(x) \times \eta(t) - \chi \times v(t) + CI \times \left(\frac{\lambda}{L} \right)^4 \times \phi(x) \times \dot{\eta}(t) + m \times \phi(x) \times \ddot{\eta}(t) = -m \frac{d^2 w_b(x,t)}{dt^2} + f_m \times \phi^{ii}(x) \times \eta(t) \tag{2.66}$$

Multiplying the above equation by eigenfunction $\phi(x)$ and then putting $\int_0^L \phi^2(x)\,dx = 1$ the equation reduces to

$$YI \times \left(\frac{\lambda}{L} \right)^4 \times \eta(t) + CI \times \left(\frac{\lambda}{L} \right)^4 \times \dot{\eta}(t) + m \times \ddot{\eta}(t) - \chi \times v(t) = -m \times \frac{d^2 w_b(x,t)}{dt^2} \times \int_0^L \phi(x)\,dx + f_m \times \eta(t) \times \int_0^L \phi(x) \times \phi^{ii}(x)\,dx \tag{2.67}$$

The equivalent electrical equation as mentioned previously is

$$\frac{C_p}{2}\frac{dv(t)}{dt}+\frac{v(t)}{R_l}-\kappa\frac{d\eta(t)}{dt}=0 \tag{2.68}$$

The above two equations (2.67) and (2.68) are coupled mechanical and electrical equations respectively. By using previously mentioned state variables in eq. (2.44), the above two second order equations can be converted into multiple first order form as given below.

$$\dot{z}_1(t)=z_2(t) \tag{2.69}$$

$$\dot{z}_2(t)=-\ddot{w}_b(t)\times\left[\int_0^L\phi(x)dx\right]+\frac{f_m}{m}\times\left[\int_0^L\phi(x)\phi^{ii}(x)dx\right]z_1(t)-\left(\frac{YI}{m}\right)\times\left(\frac{\lambda}{L}\right)^4 z_1(t)-\left(\frac{CI}{m}\right)\left(\frac{\lambda}{L}\right)^4 z_2(t)+\left(\frac{\chi}{m}\right)z_3(t) \tag{2.70}$$

$$\dot{z}_3(t)=\left(\frac{2\kappa}{C_p}\right)z_2(t)-\left(\frac{2}{R_l\times C_p}\right)z_3(t) \tag{2.71}$$

The above three equations can be simulated in Matlab by using Runge-Kutta solver to get the displacement as well as induced voltage.

CHAPTER 3

RESULTS AND DISCUSSION

This chapter includes the results obtained during the analysis. Effects of various parameters of the energy harvester on the output power generated are described one by one.

3.1 Lumped parameter Modeling

In the single degree of freedom lumped parameter model, piezoelectric bimorph energy harvester is considered to have a mass, stiffness and damping. A sinusoidal base excitation is applied to the cantilever and equivalent mass of the beam is considered. A series connection from the piezolayer is considered for illustration.

3.1.1 Effect of substrate materials of cantilever

Copper and Aluminum are used as substrate materials in two independent cases by keeping PZT-5A as a piezoelectric material. The chemical representation of PZT-5A is Pb $[Zr_xTi_{1-x}]$ O_3 $(0\leq x\leq 1)$. It is conventionally used piezoelectric material with excellent piezoelectric properties. The material properties of substrate as well as piezolayer are summarized in Table 3.1 below.

Table 3.1 Material properties of Substrate and piezolayer

Parameter	Substrate 1 (Copper)	Substrate 2 (Aluminum)	Piezolayer (PZT-5A)
Length (mm)	L=55	L=55	L=55
Width (mm)	B=5	B=5	B=5
Thickness (mm)	h_s =1	h_s =1	h_p =2
Density (kg/m^3)	ρ_s =8900	ρ_s =2700	ρ_p =7750

Elastic modulus (GPa)	Y_s =125	Y_s =72	Y_p =61
Electromechanical coupling coefficient (N/V)	---	---	θ =1.496×10^{-5}
Permittivity constant (nF/m)	---	---	E_{33} =13.3
Piezoelectric constant (m/V)	---	---	d_{33} =390×10^{-12}

The material and geometric properties of tip mass are shown in Table 3.2.

Table 3.2 Tip Mass geometrical properties

Parameter	Value
Length (mm)	L_m =10
Width (mm)	B_m =5
Thickness (mm)	h_m =7
Density (kg/m^3)	ρ_m =7800

The additional magnetic force is provided to the proposed piezoelectric energy harvester along with the base excitation. Some of the important magnetic parameters are summarized in Table 3.3.

Table 3.3 Electromagnetic parameters [29]

Parameter	Value
Distance between magnets (mm)	D_0 = 8
Permeability of the medium (H/m)	τ_0 = 4π×10^{-7}
Surface flux	β = 1.4

This model is simulated for two cases namely aluminum as a substrate with PZT-5A as a piezolayer (blue line) and copper as a substrate with PZT-5A as a piezolayer (red line). In order to solve the coupled differential equations with displacement and voltage as variables the fourth order Runge-Kutta numerical time marching method is used. The equivalent mass of the beam and stiffness are first computed and a program is developed in Matlab for obtaining the solution. A part of Matlab code and corresponding output results are presented below.

PART OF MATLAB CODE WITH RUNGE-KUTTA SOLVER

```
Meq=((33/140)*Mb)+Mt; % equivalent mass
Ib=(w*(tb^3))/12; % MI of beam,
Ip=(w*(tp^3))/12; % MI of piezolayer
EI= (Eb*Ib)+(2*w*Ep*(H^3)/3)-(Ep*Ip);  % flexural rigidity
Keq=(3*EI)/(l^3);  % equivalent stiffness
Wn=(Keq/Meq)^0.5; % natural frequency
Ceq=2*D*Meq*Wn; % equivalent damping
S=Mt/Mb;
U=(S^2+0.603*S+0.08955)/(S^2+0.4637*S+0.0571); % Correction factor
R=1/(Wn*CS); % load resistance
V= (ml*mw*mt); % volume of the magnet
m1= (2*B*V)/Tm; % moment of magnetic dipole
m2=-m1; % moment of magnetic dipole
Fm=-(3*Tm*m1*m2)/(pi*(md^4)); % magnetic force
f(1)= x(2);
f(2)= -(Ceq/Meq)*x(2)-(Keq/Meq)*x(1)-(Tf/Meq)*x(3)+Fm+(U*500*sin(10*t));
f(3)= (Tf/CS)*x(2)-(1/(R*CS))*x(3);
f=[f(1);f(2);f(3)];
clear all
clc
x=[0,0,0]; % Initial conditions
t0=0; % initial time
tf=0.01; % finsl time
tspan=linspace(t0,tf,100000); % timespan
[t,x]=ode45('lumped1',tspan,x); % function call
plot(t,x(:,3),'-b','LineWidth',2);
xlabel('time');
ylabel('Induced Voltage');
grid on
```

The Fig 3.1 shows time domain history of induced voltage. It is clear that the aluminum has much sensitivity compared to copper.

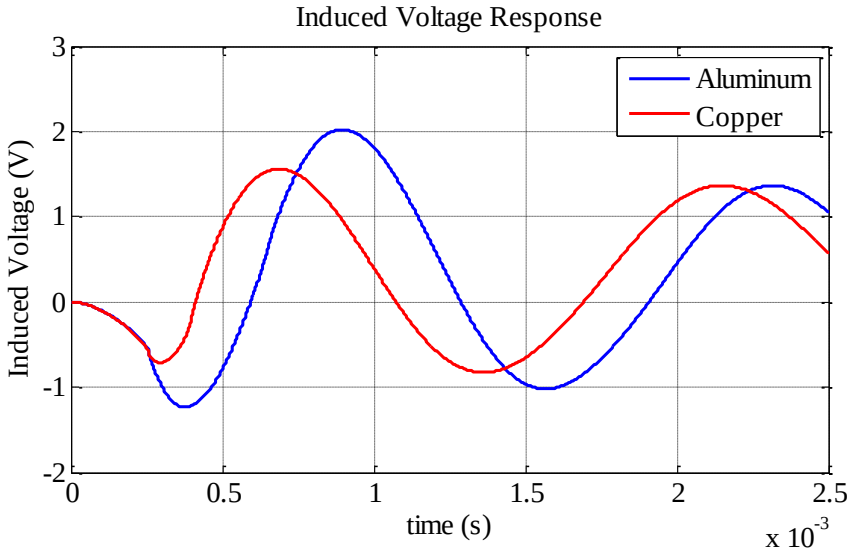

Fig. 3.1 Induced voltage response with time ($R_l = 1 \times 10^7 \Omega$)

Fig. 3.2 represents tip mass amplitude response with respect to resonance frequency. It can be seen that for aluminum case the maximum amplitude is approximately 0.0071 mm at resonance frequency 687.21Hz and for copper it is 0.0055 mm at the resonance frequency of 646.47Hz.

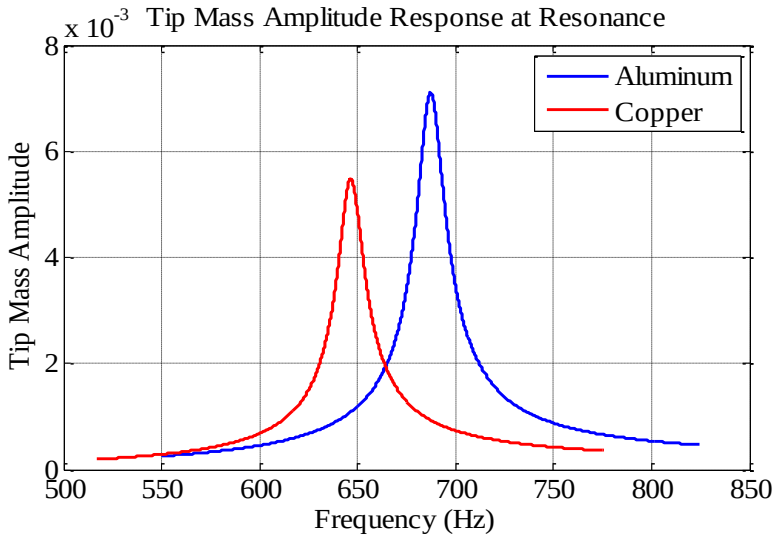

Fig. 3.2 Tip mass amplitude response at resonance frequency

Fig. 3.3 represents the FFT of induced voltage response. It can be seen that for aluminum and approximate voltage generated at the maximum amplitude is 2.05 V and 1.6 V respectively.

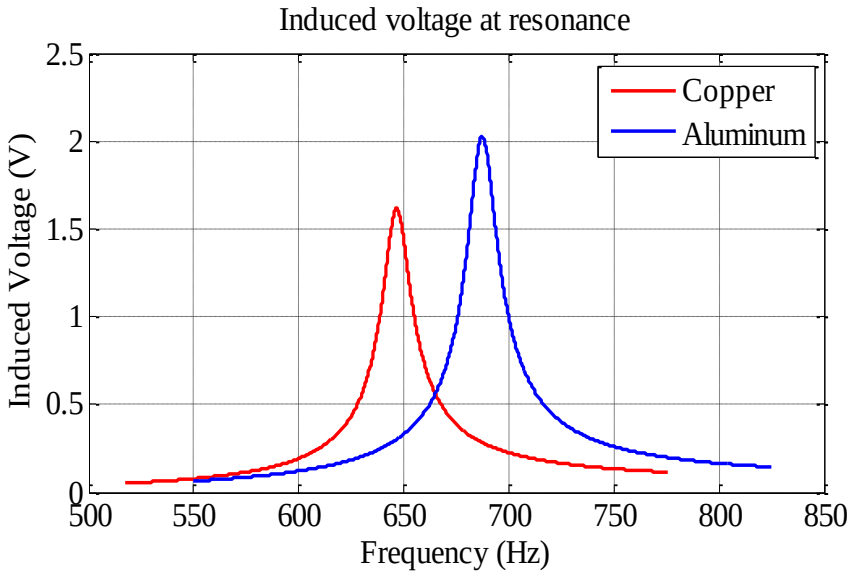

Fig. 3.3 Induced voltage response at resonance frequency

Induced voltage also depends upon load resistance and hence Fig. 3.4 shows the variation of amplitude of voltage at resonance frequency with respect to load resistance. It can be seen that after 1×10^7 Ω of load resistance, the induced voltage amplitude becomes constant.

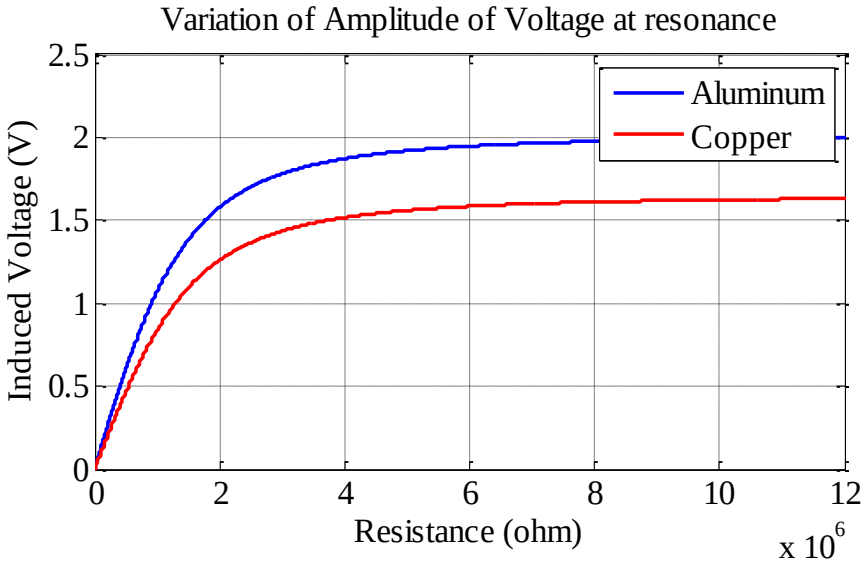

Fig. 3.4 Variation of amplitude of voltage at resonance

The equivalent output Power FRF is shown in Fig. 3.5. The maximum power harvested for copper as well as aluminum case at resonance is 0.95 μw and 1.25 μw respectively.

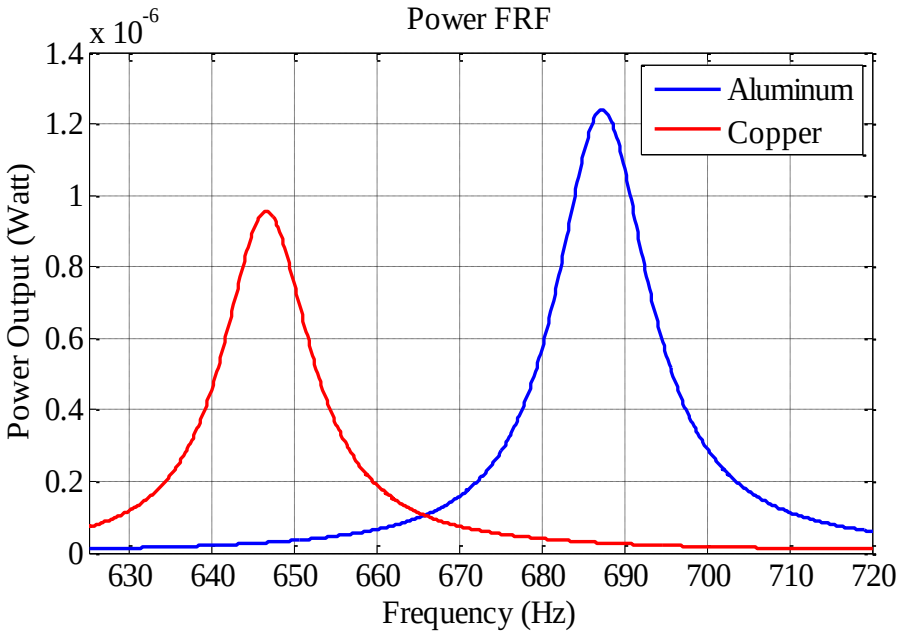

Fig. 3.5 Power FRF at resonance

3.1.2 Effect of piezoelectric material

In this section, two different piezoelectric materials are considered independently. Conventional PZT-5A is well known piezoelectric material but it is hazardous. Polyvinylidene Fluoride (PVDF) is semi-crystalline high-molecular polymer composite material and it is recently developed as a piezoelectric material. The chemical formula of PVDF is - $(C_2H_2F_2)$ n - and Curie temperature is 110^0 C hence it can be used at elevated temperature conditions. PVDF produces exponentially high voltage and possesses excellent piezoelectric properties. The geometric and material properties of PZT-5A and PVDF along with aluminum (Substrate) are summarized in Table 3.4. The geometric properties of tip mass and important magnetic properties of magnet are same as previous case.

Table 3.4 Material properties of substrate and piezolayer [35]

Parameter	Substrate (Aluminum)	Piezolayer (PZT 5A)	Piezolayer PVDF
Length (mm)	L=55	L=55	L=55
Width (mm)	B=5	B=5	B=5
Thickness (mm)	h_s=1	h_s=2	=2
Density (kg/m3)	ρ_s=2700	ρ_p=7750	ρ_p=1750
Elastic modulus (GPa)	Y_s=72	Y_p=61	Y_p=2.8
Electromechanical coupling coefficient (N/V)	---	θ=1.496×10^{-5}	θ=7.5×10^{-5}
Permittivity constant (nF/m)	---	E_{33}=13.3	E_{33}=112.2
Piezoelectric constant (m/V)	---	d_{33}=390×10^{-12}	d_{33}=-33×10^{-12}

The two cases considered in this section has aluminum as substrate material and two different independent piezoelectric materials are PZT-5A (red) and PVDF (blue). The resonance frequency of the energy harvester depends upon material as well as geometric properties of substrate and piezoelectric material. PVDF is more flexible than PZT-5A and hence it will deflect more giving lesser resonance frequency. The resonance frequency by considering PVDF as a piezolayer is 161.8Hz. For PZT-5A case, the resonance frequency is 687.21Hz. The tip mass amplitude response for both the cases is shown in the Fig. 3.6. It can be seen that the maximum amplitude for PVDF is 0.036 mm and for PZT-5A is 0.007 mm and hence former will definitely induce more voltage than later.

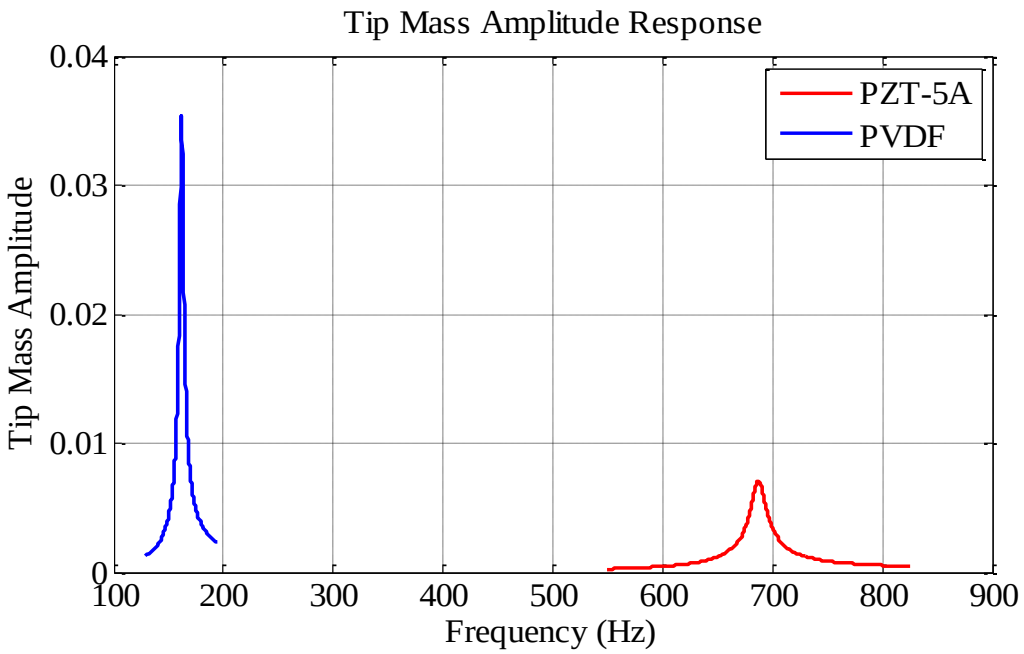

Fig. 3.6 Tip mass amplitude response at resonance frequency

The Fig. 3.7 represents induced voltage response at load resistance of $1\times10^{7}\,\Omega$. It can be seen that the maximum voltage induced by PVDF case is about 10.01 V and PZT-5A case is about 2.05 V.

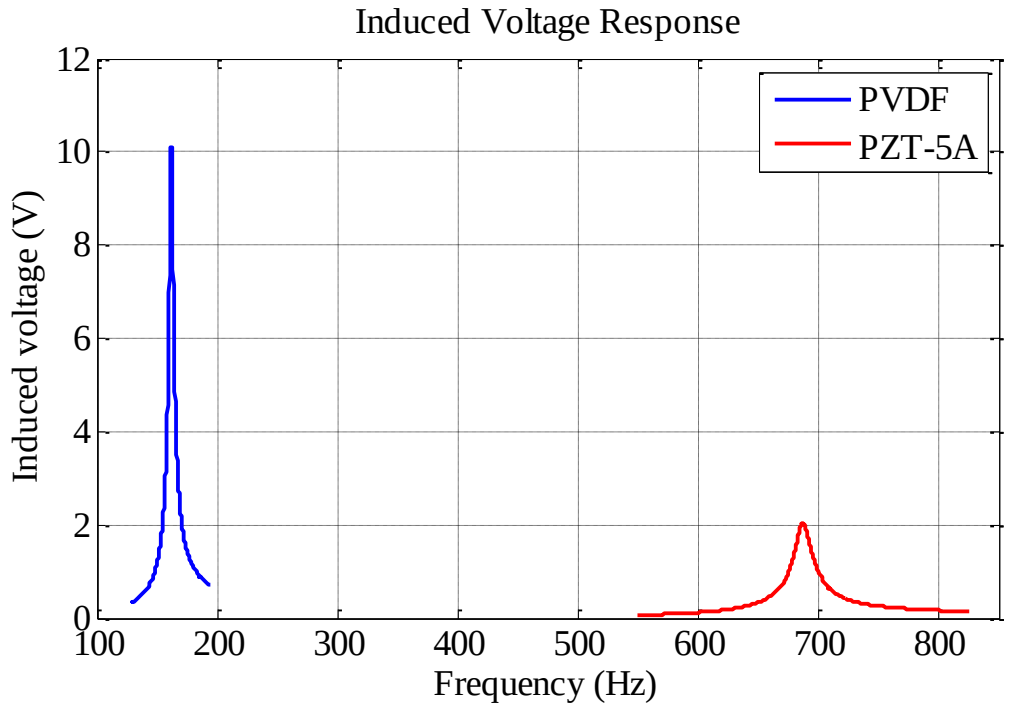

Fig. 3.7 Induced voltage response at resonance frequency

Fig. 3.8 represents variation of amplitude of induced voltage at resonance with respect to load resistance. It can be seen that the amplitudes with PVDF are much higher compared to PZT-5A.

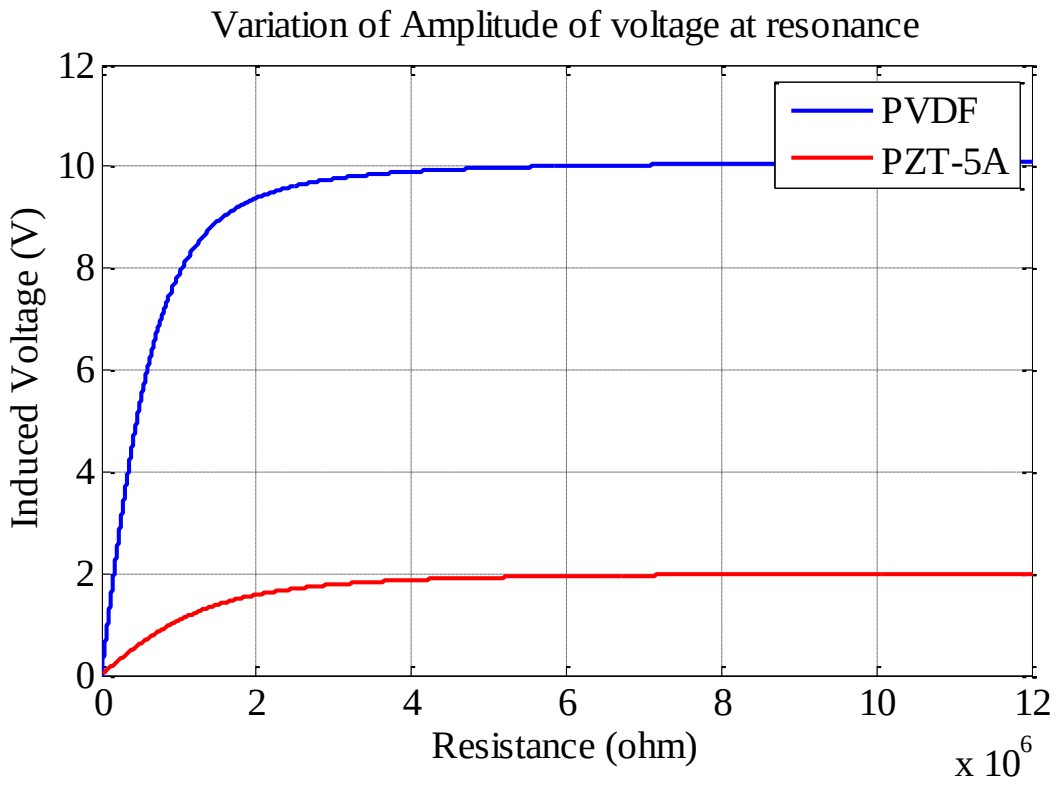

Fig. 3.8 Variation of amplitude of voltage at resonance

The Power FRF is shown in Fig. 3.9. It can be seen that for PZT-5A as well as PVDF case the power output is 1.25 μw and 3.1 μw respectively at resonance frequency.

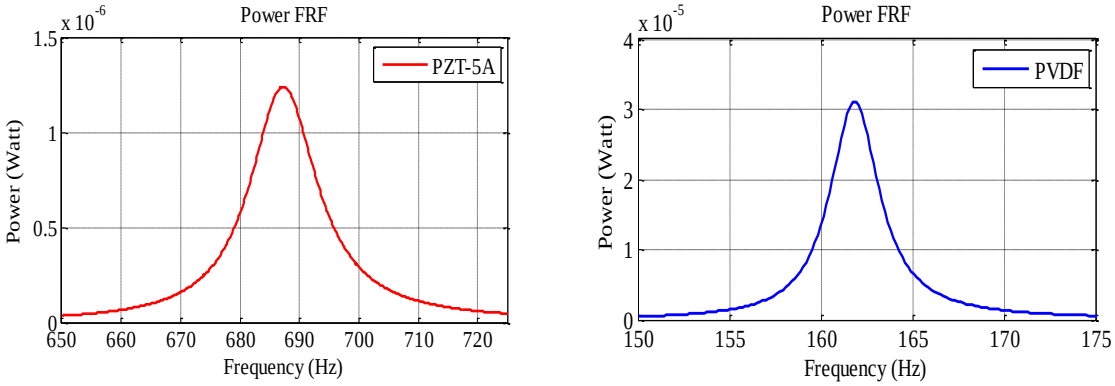

Fig. 3.9 Power FRF at resonance

3.1.3 Effect of tip mass on the power

If the tip mass is varied then there is equivalent change in induced voltage and power. In this section, aluminum is considered as a substrate material with PZT-5A as piezolayer. Here tip mass is varied by keeping all the other parameters constant and its effect on power output is studied. From Fig. 3.10 it can be seen that, as tip mass increases the resonance frequency decreases and power output increases. For the tip mass 4.5 g, the maximum power harvested is 6.7 μw at the resonance frequency of 657.5 Hz.

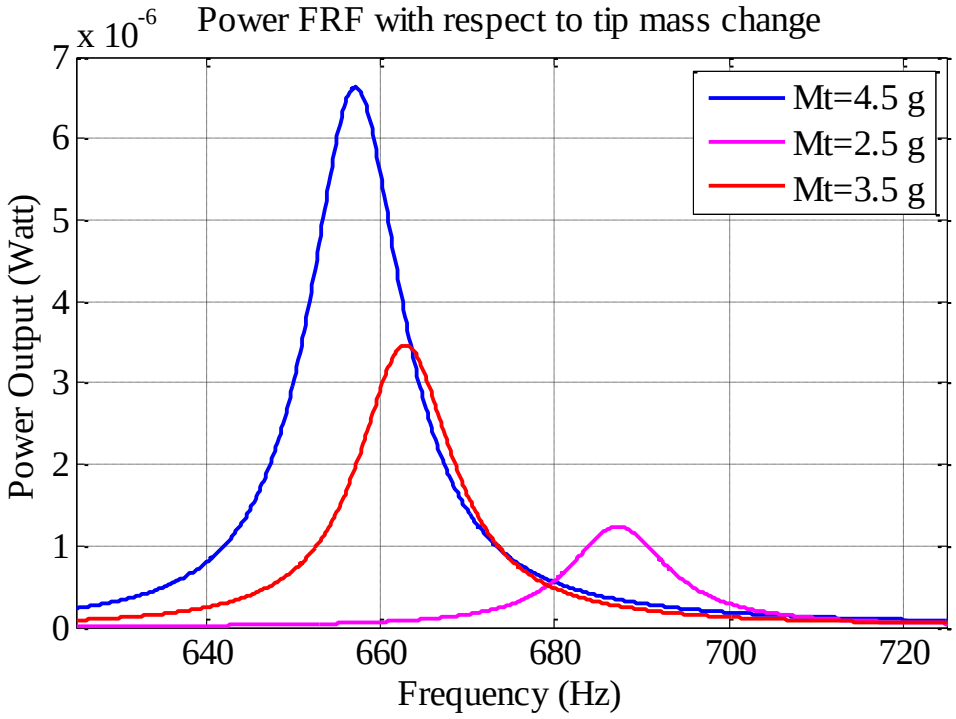

Fig. 3.10 Power FRF with respect to change in tip mass

3.1.4 Effect of distance between fixed magnet and tip mass

If the distance between fixed magnet and tip mass is varied then there is change in induced voltage and hence the output power. Here, aluminum is considered as a substrate and PZT-5A is taken as a piezoelectric material. Fig. 3.11 represents the time domain history of induced voltage

response with variation in distance D_0. It is observed that induced voltage is maximum at distance (D_0)=0.015 mm and it is equal to 2.265 V. It should be noted that if the distance is increased or decreased from this value the induced voltage decreases.

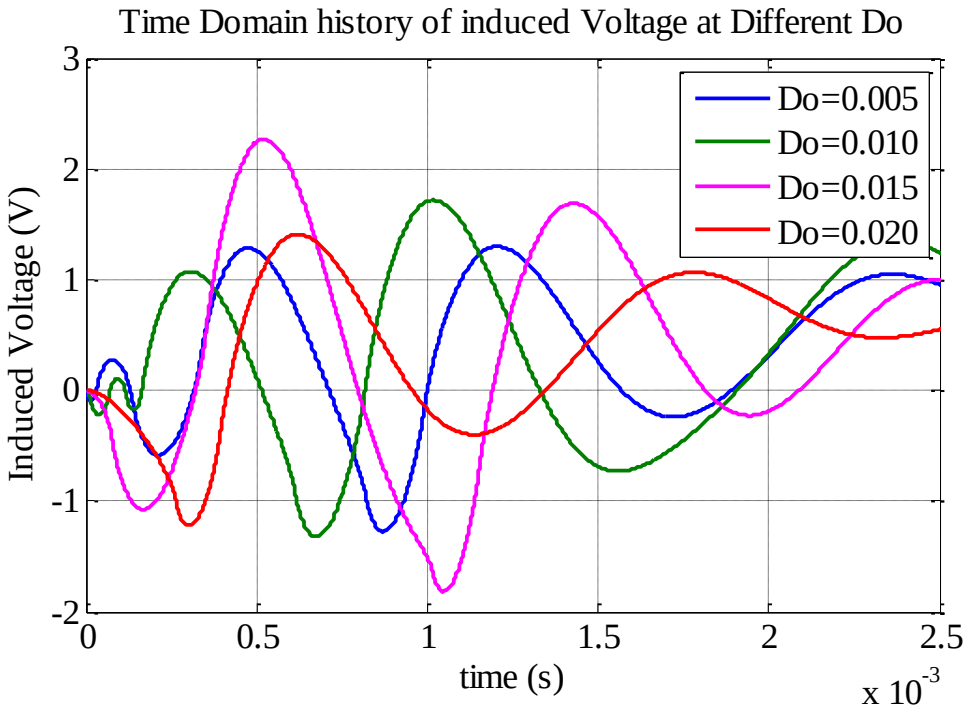

Fig. 3.11 Induced voltage response with variation in distance D_0

3.1.5 Effect of random base excitation

In this section, random base excitation in the form of Gaussian white noise is provided and its effect on displacement and induced voltage is studied. Here, the substrate material in the form of aluminum and piezoelectric material in the form of PZT-5A is considered. The equivalent power of 2 decibels is given to the random excitation. Fig. 3.12 represents time domain history of displacement corresponding to the following part of the Matlab code.

PART OF MATLAB CODE WITH RUNGE-KUTTA SOLVER

```
%%%%%% Calculation of Additional magnetic force
V=(ml*mw*mt); % Volume of the magnet
m1=(2*B*V)/Tm; % moment of magnetic dipole
m2=-m1; % moment of magnetic dipole
F=-(3*Tm*m1*m2)/(pi*(md^4)); % magnetic force
%%%%%% base excitation
mm=1;
nn=1;
pp=2;
qq= wgn(mm,nn,pp); % Gaussian White Noise generation
%%%%%% Defining Coupled equations
f(1)=x(2);
f(2)=-(Ceq/Meq)*x(2)-(Keq/Meq)*x(1)-(Tf/Meq)*x(3)+(3*Tm*m1*m2)/(pi*(x(1)+md^4))+qq;
f(3)=(Tf/CS)*x(2)-(1/(R*CS))*x(3);
f=[f(1);f(2);f(3)];
```

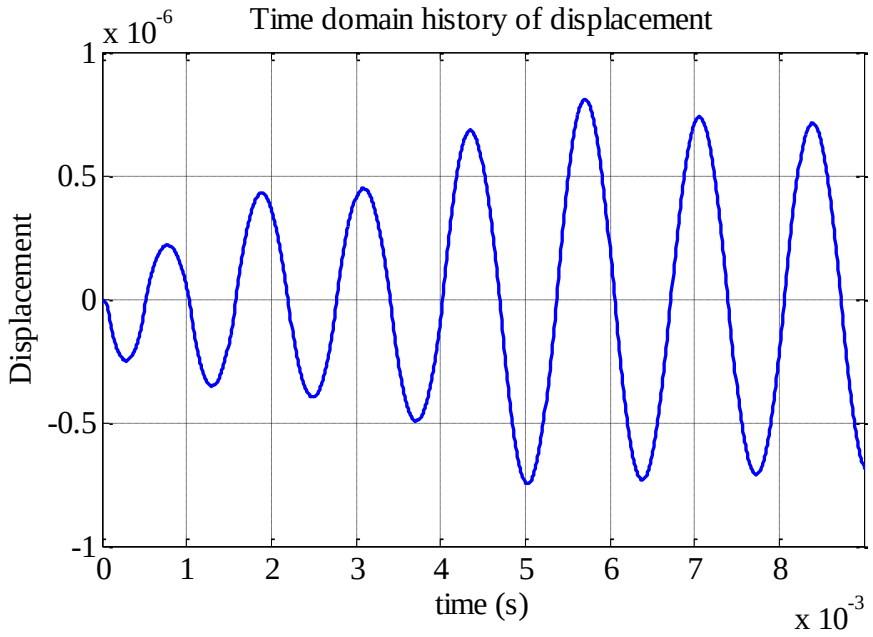

Fig. 3.12 Time domain history of displacement

The corresponding induced voltage is represented in Fig. 3.13 given below. It can be seen that for the given random excitation, the maximum induced voltage is 1.45 V.

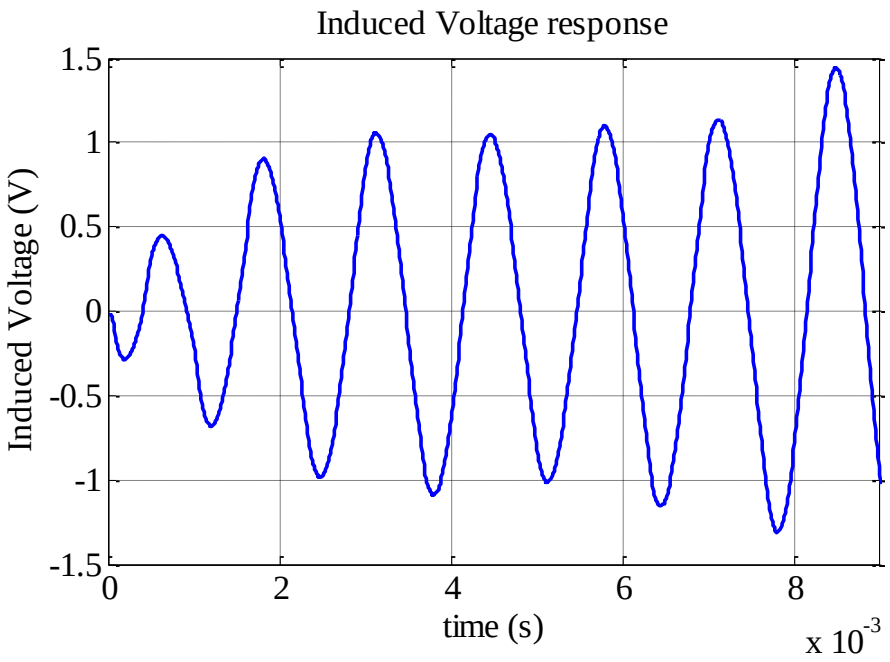

Fig. 3.13 Induced voltage response

3.2 Continuous system modeling

Distributed parameter model is reliable but at the same time it is computationally cumbersome. It is difficult to obtain the exact solution but the results obtained by using distributed parameter model are very close to exact solution. The distributed parameter bimorph piezoelectric energy harvesting model is solved by using Euler-Bernoulli beam theory in previous chapter. The coupled second order differential equations are decoupled into multiple first order differential form which then can be solved using Runge-Kutta numerical solution. The material and geometric properties of substrate and piezolayer are summarized in the Table 3.5 below.

Table 3.5 Material properties of substrate and piezolayer [34]

Parameter	Substrate (Aluminum)	Piezolayer (PZT-5A)
Length (mm)	L=30	L=30

Width (mm)	L=5	L=5
Thickness (mm)	h_s =0.05	h_p =0.15
Density (kg/m3)	ρ_s =2700	ρ_p =7750
Elastic modulus (GPa)	Y_s =72	Y_p =61
Electromechanical coupling coefficient (N/V)	---	θ =1.496×10^{-5}
Permittivity constant (nF/m)	---	E_{33} =13.3
Piezoelectric constant (C/m^2)	---	e_{31} =-10.4

The material and geometric properties of tip mass and some of the important properties of additional magnetic field are same as pervious lumped parameter case.

PART OF MATLAB CODE WITH RUNGE-KUTTA SOLVER

```
Mt=(ml*mw*mt*mq); % tip mass m=B*((qs*Hs)+(2*qp*Hp)); % mass/length of beam
YI=(2*B/3)*((Ys*(Hs^3)/8)+Yp*((Hp+(Hs/2))^3-(Hs^3/8)));% Equivalent stiffness
omg=lm^2*(YI/(m*(L^4)))^0.5;
syms x
Sr=((sin(lm)-sinh(lm))+((lm*Mt)/(m*L))*(cos(lm)-cosh(lm)))/((cos(lm)-cosh(lm))-((lm*Mt)/(m*L))*(sin(lm)-
sinh(lm)));
fi=Ar*(cos(lm*x/L)-cosh(lm*x/L)+Sr*(sin(lm*x/L)-sinh(lm*x/L))); % mass normalized Eigen function
IMP=diff(fi,x); % differentiation of Eigen function
fr=-m*((G*INTEG1)+(H*INTEG2))-((Mt*D)*(G+(L*H))); % total mechanical force
%%%%%% coupled electrical circuit equation
Cp=(E33*B*L)/Hp; % internal capacitance
kr=((E31*(Hp+Hs)*B)/2)*d; % dependent current source
Rl=1000000; % load resistance
V= (ml*mw*mt); % volume of the magnet
m1= (2*B*V)/Tm; % moment of magnetic dipole
m2=-m1; % moment of magnetic dipole
Fm=-(3*Tm*m1*m2)/(pi*(md^4)); % magnetic force
%%%%%% Representation of equations
t=tt;
AA=vpa(fr+Fm-(19.3*z(2))-((omg^2)*z(1))+(xrs*z(3)));
AA=subs(AA);
f(1)=z(2);
```

```
f(2)=AA;
f(3)=(-2/(Rl*Cp))*z(3)-(2*kr/Cp)*z(2);
f=[f(1);f(2);f(3)];

clear all
clc
z=[0,0,0]'; % initial conditions
Rl=1000000; % load resistance
t0=0; % initial time
tf=0.5; % final time
 [t,z]=ode45('continuous',[0,0.5],z); % R-K solver
plot(t,z(:,3),'-b','linewidth',2);
xlabel('time(s)');
ylabel('Induced Voltage (V)');
grid on
```

In order to reduce the partial differential equations into Ordinary Differential Equations form, single mode approximation is considered and Matlab symbolic mathematics toolbox is employed to integrate and simplify the terms. The resultant Ordinary Differential Equations in time variable are solved using Runge-Kutta solver in Matlab software. The Fig. 3.14 represents the time domain history of tip mass displacement.

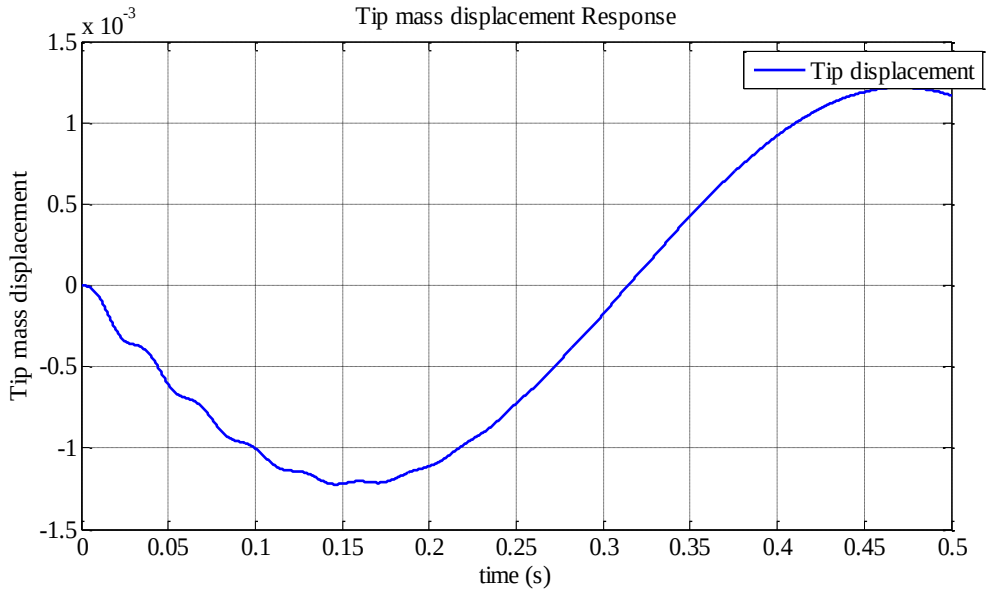

Fig. 3.14 Tip mass displacement Response

The corresponding induced voltage is shown in the Fig. 3.15 below. It can be seen that the maximum voltage obtained here is about 0.033 V or 33 mV.

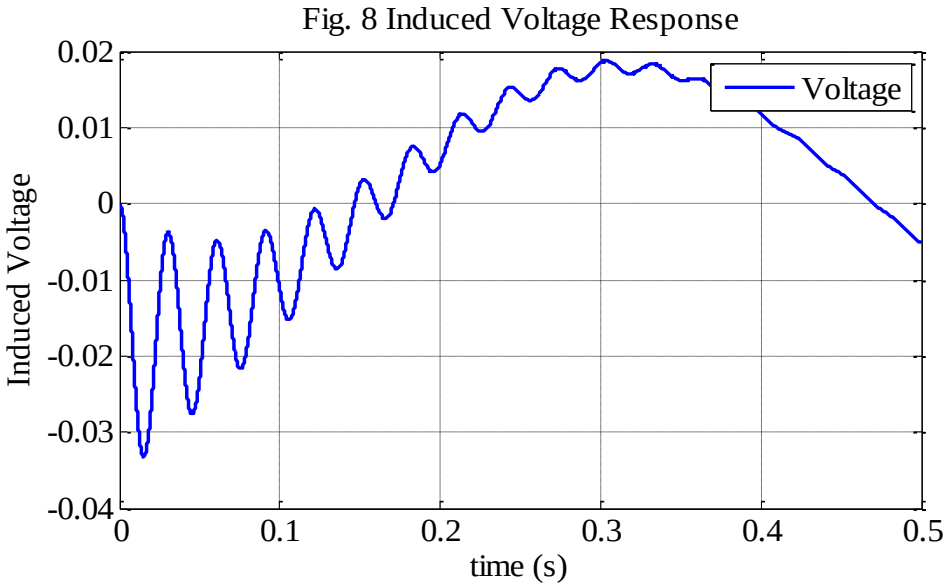

Fig. 3.15 Induced Voltage Response

From the Fig. 3.16, it can be seen that the resonance frequency of the proposed energy harvester is 33.3 Hz and the maximum energy harvested is about 2.201×10^{-8} watt.

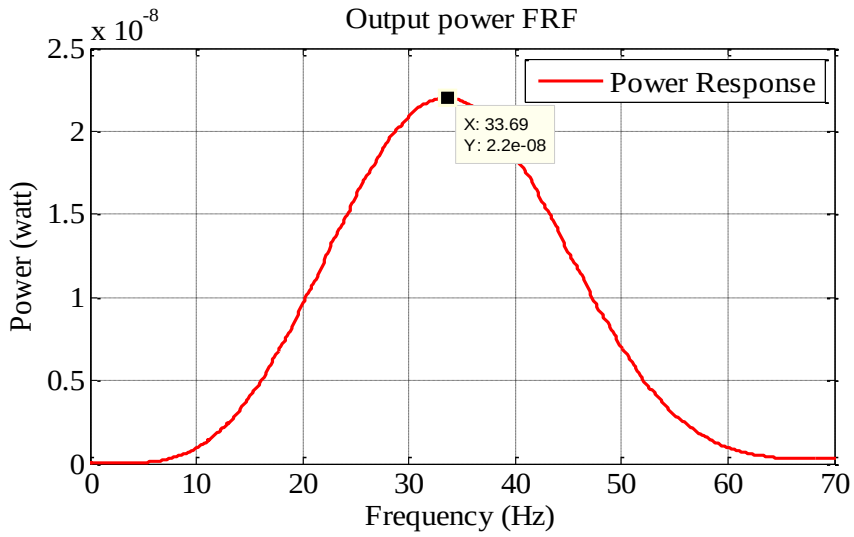

Fig. 3.16 Output power FRF at resonance

3.3 Experimental Work

The proposed bimorph cantilever beam piezoelectric energy harvester with tip mass and additional magnetic field is tried to fabricate in laboratory. The cantilever beam substrate material should be electrically conductive and hence Aluminum is taken as substrate material along with mild steel as a tip mass. The cantilever beam and tip mass dimensions are precisely obtained by performing various operations like grinding, filing, etc. The geometric dimensions of substrate and tip mass are summarized in Table 3.6 below.

Table 3.6 Geometric properties of substrate and tip mass

Parameter	Substrate (Aluminum)	Tip mass (Mild steel)
Length (mm)	L=62	L_m =15.70
Width (mm)	B=14.5	B_m =7.10
Thickness (mm)	h_s =0.7	h_m =5.90

The tip mass is fixed to the cantilever beam by using feviquick as adhesive and adding mild steel particles for giving the strength. It is planned to patch the Barium Zirconate Titanate (BZT) as a piezolayer over both the thickness directions of cantilever beam. But due to some limitations of available BZT in laboratory only the aluminum cantilever beam with mild steel tip mass is experimentally analyzed. To find out the first mode resonance frequency of aluminum cantilever beam with tip mass, base excitation is provided by using vibration shaker and additional magnetic force is provided at tip by using fixed external magnets. Fig. 3.17 shows the cantilever beam with tip mass.

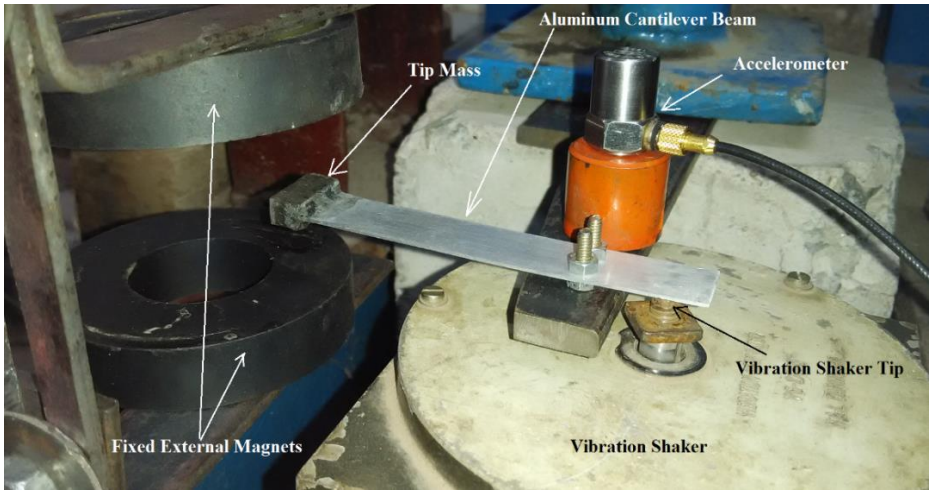

Fig. 3.17 Cantilever beam with tip mass in magnetic field

The complete experimental set-up contains following devices-

1. Vibration shaker
2. Function generator
3. Power amplifier
4. Accelerometer
5. Digital oscilloscope

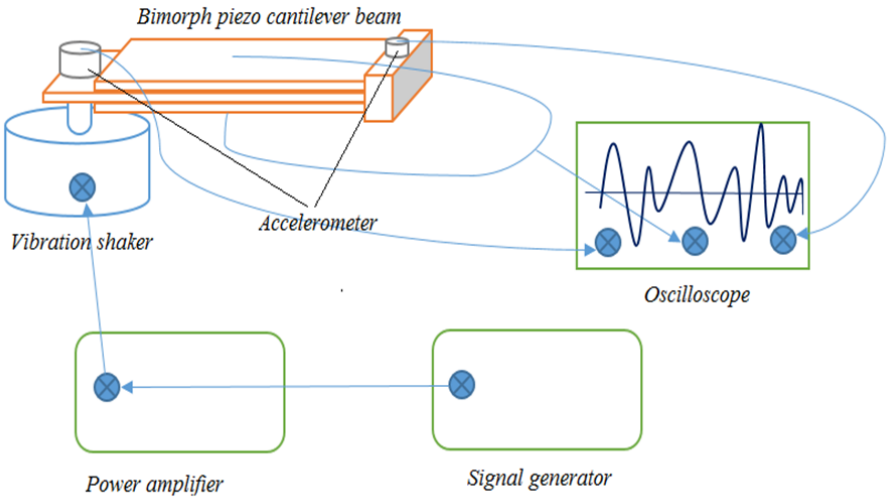

Fig. 3.18 Experimental Set-up

These devices are connected as shown in Fig. 3.18 above so as to provide the base excitation to the cantilever beam and also to measure the input base vibrations at the fixed end as well as output vibrations from free end. Oscilloscope is the electronic display device. There are two channels in the oscilloscope, channel 1 shows the base excitation provided at the fixed end of cantilever beam and channel 2 gives displacement of tip mass. Both the outputs of the oscilloscope are in mV. The corresponding oscilloscope screen shot is shown in Fig. 3.19 below.

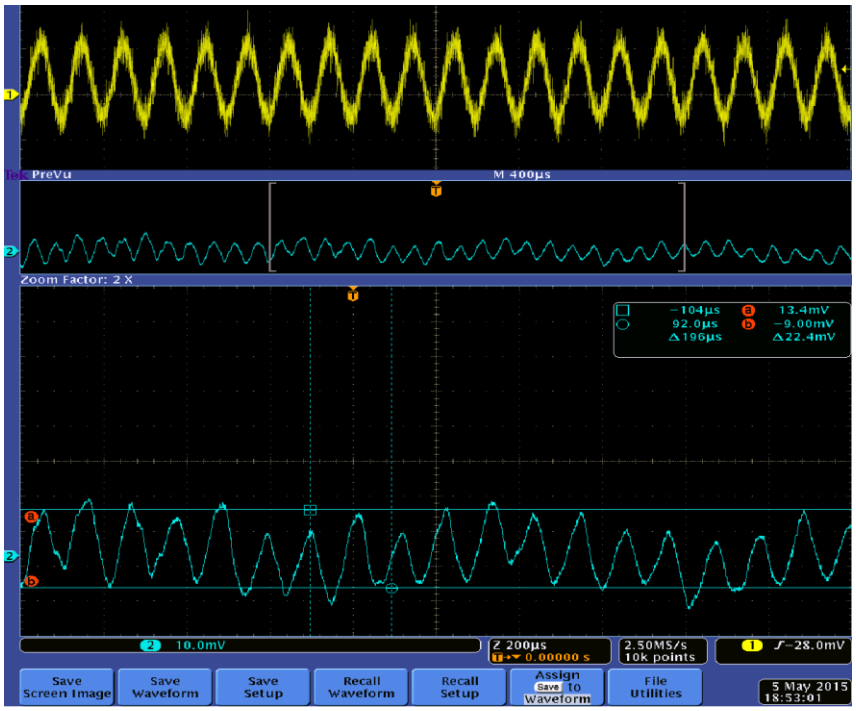

Fig. 3.19 Oscilloscope screen shot

The oscilloscope reading is recorded and first mode resonance frequency of the cantilever beam with mild steel tip mass is experimentally determined. Fig. 3.20 shows the tip mass amplitude response of proposed cantilever beam with the resonance frequency 97 Hz.

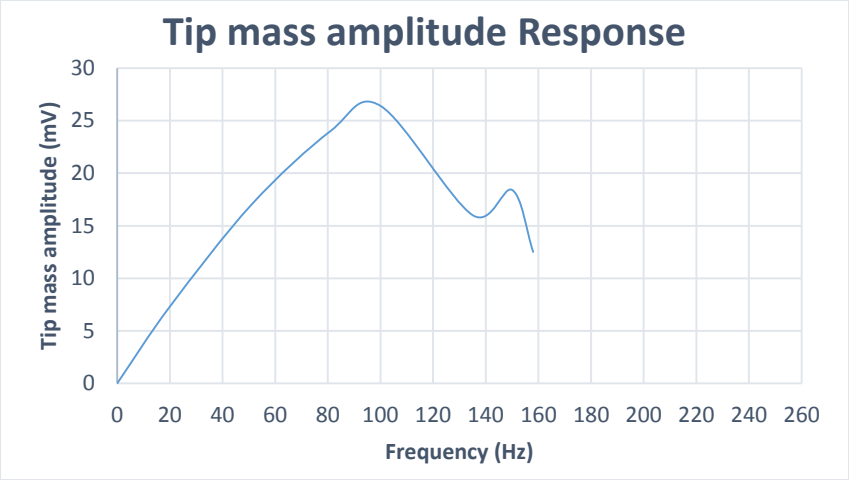

Fig. 3.20 Tip mass amplitude response

CHAPTER 4

CONCLUSIONS

This chapter includes the overall summary of all the research topics presented in this thesis. The chapter is concluded by the future scope.

4.1 Summary

The bimorph cantilever beam piezoelectric energy harvester with magnetic tip was modeled by considering lumped parameter model and distributed model. The proposed energy harvester was excited in additional magnetic field for broadband energy harvesting performance. Using ANSYS model the natural frequencies of piezoelectric cantilever are obtained. The effects of various parameters of energy harvester system on induced voltage and output power were studied. In the first case, aluminum and copper are considered as substrate materials independently with PZT-5A as a piezolayer. It is observed that aluminum is giving more reliable results as it is flexible than copper. In the second case, PZT-5A and PVDF are considered as a piezolayer materials independently by considering aluminum as a substrate material. Obviously polymer composite PVDF material is giving more reliable results as compared to PZT-5A. The effect of tip mass on the power harvested is also studied and it is concluded that with the increase in tip mass, resonance frequency reduces and output power increases. The distance between tip magnet and one of the side of fixed magnet also influences the induced voltage and hence power output of the harvester. The simulation study shows that the optimum distance (D_0) for proposed energy harvester system is 15 mm. Random base excitation in the form of Gaussian white noise is also provided to the Single-degree of freedom lumped parameter model.

The continuous system model is employed by considering Euler-Bernoulli beam theory. The Galerkin's technique is used to reduce the equations of motion with first mode approximation. The experimental analysis is attempted for proposed energy harvester. In this regard, aluminum cantilever beam with mild steel tip mass is fabricated without piezolayer and it is excited in additional magnetic field for the purpose of finding out resonance frequency. From experimental investigation resonance frequency is found to be 97 Hz.

4.2 Future Scope

The multi-mode Galerkin's approximation is more reliable and it can be tried as a future work. The proposed distributed parameter energy harvester is modeled only by using Euler-Bernoulli beam theory but the more accurate modeling can be done by using Thimoshenko as well as Rayleigh beam theory. Finite element modeling results are to be obtained and validated. The effect of different parameters of energy harvesting system on the induced voltage and power will be deeply studied so as to get the optimum performance of the system. Finally, the experimental work needs to be carried out by mounting the piezoelectric patches on the beam and preparing an electric circuit to estimate the amount of power developed for these specifications.

REFERENCES

[1] C. B. Williams and R. B. Yates, 'Analysis of microelectronic generators for microsystems', Sensors and Actuators, 52 (1996) 8-11.

[2] S. P. Beeby, M. J. Tudor and N. M. White, 'Energy harvesting vibration sources for microsystems applications', Measurement Science and Technology, 17 (2006) 175-195.

[3] K. A. Chennault, N. Thambi and A. M. Sastry, 'Powering MEMS portable devices - a review of non-regenerative and regenerative power supply systems with special emphasis on piezoelectric energy harvesting systems', Smart Materials and Structures, 17 (2008) 1-33.

[4] L. Tang and Y. Yang, 'A multiple degree of freedom piezoelectric energy harvesting model', Journal of Intelligent Materials Systems and Structures, 23(14) (2012) 1631-1647.

[5] Hao Wu, Lihua Tang, Yaowen Yang and Chee Kiong Soh, 'A novel two-degrees-of-freedom piezoelectric energy harvester', Journal of Intelligent Material Systems and structures, 24(3) (2012) 357-368.

[6] H. K. Joo and T. P. Sapsis, 'Performance Measures for single degree of freedom energy harvesters under stochastic excitation', Journal of Sound and Vibration, 333 (2014) 4695-4710.

[7] A. Khalatkar, V. K. Gupta, and A. Agrawal, 'Analytical, FEA, and Experimental Comparisons of Piezoelectric Energy Harvesting Using Engine Vibrations', Smart materials Research, 22 (2014) 1-8.

[8] Y. C. Shu and C. I. Lein, 'Analysis of power output from piezoelectric energy harvesting system', Smart Materials and Structures, 15 (2006) 1499-1512.

[9] D. Zhu, M. J. Tudor and S. P. Beeby, 'Strategies for increasing the operating frequency range of vibration energy harvesters: A review', Measurement Science and Technology, 21 (2010) 1-29.

[10] W. G. Ali and S. W. Ibrahim, 'Power analysis for piezoelectric energy harvester', Energy and Power Engineering, 4 (2012) 496-505.

[11] B. Ando, S. Baglio, F. Maiorca and C. Trigona, 'Analysis of two dimensional, wide-band, bi-stable vibration energy harvester', Sensors and Actuators A: Physical 202 (2013) 176-182.

[12] W.A. Jiang and L. Q. Chen, 'An equivalent linearization technique for nonlinear piezoelectric energy harvesters under Gaussian white noise', Common Nonlinear Sci Number Simult, 19 (2014) 2897-2904.

[13] A. Erturk and D. J. Inman, 'A Distributed Parameter Electromechanical Model for Cantilevered Piezoelectric Energy Harvesters', Journal of vibration and Acoustics, 130 (4) 2008 1-13.

[14] A. Erturk and D. J. Inman, 'On mechanical modelling of cantilevered piezoelectric vibration energy harvesters', Journal of Intelligent Material Systems and Structures, 19 (2008) 1311-1325.

[15] A. M. Wickenheiser, 'Design Optimization of Linear and Non-Linear Cantilevered Energy Harvesters for Broadband Vibrations', Journal of Intelligent Material Systems and structures, 22 (2011) 2013-2025.

[16] A. Abdelkefi, A. H. Nayfeh and M. R. Hajj, 'Global nonlinear distributed-parameter model of parametrically excited piezoelectric energy harvesters', Nonlinear Dynamics, 67 (2012) 1147-1160.

[17] N. H. Diyana, A. G. A. Muthalif, M. N. Fakhazan and A. N. Nordin, 'Vibration energy harvesting using and comb-shaped piezoelectric beam structures: Modeling and Simulation', Procedia Engineering, 41 (2012) 1228-1234.

[18] X. Xiong and S. O. Oyadiji, 'Modal electromechanical optimization of cantilevered piezoelectric vibration energy harvesters by geometric variation', Journal of Intelligent Material Systems and structures, 25(10) (2013) 1177-1195.

[19] M. N. Fakhzan and Asan G. A. Muthalif, 'Harvesting vibration energy using piezoelectric material: Modeling, simulation and experimental verifications', Mechatronics, 23 (2013) 61-66.

[20] A. H. D. Yazdi, N. Elvin, Y. Andreopoulos, 'Green's function method for piezoelectric energy harvesting beams', Journal of Sound and Vibration, 333 (2014) 3092–3108.

[21] A. G. A. Muthalif and N. H. Diyana Nordin, 'Optimal piezoelectric beam shape for single and broadband vibration energy harvesting: Modeling, simulation and experimental results, Mechanical systems and signal processing', Mechanical Systems and Signal Processing, 54-55 (2015) 417–426.

[22] C. D. Marqui, A. Erturk and D. J. Inman, 'An electromechanical finite element model for piezoelectric energy harvester plates', Journal of Sound and Vibration, 327 (2009) 9-25.

[23] G. Wang, 'Analysis of bimorph piezoelectric energy harvesters using Thimoshenko and Euler-Bernoulli beam theory', Journal of Intelligent Material Systems and Structures, 24(2) (2012) 226-239.

[24] Eziwarman, M. F. Lumentut and I. M. Howard, 'Comparative numerical studies of electromechanical finite element vibration power harvester approaches of a piezoelectric unimorph', Advanced Intelligent Mechatronics, 45 (2014) 748-753.

[25] A. Kumar, A. Sharma, K. Rajeev, R. Vaish and V. S. Chauhan, 'Finite element analysis of vibration energy harvesting using lead-free piezoelectric material: A comparative study', Journal of Asian Ceramic Societies, 2 (2014) 138-143.

[26] Y. amini, H. Imdad and M. Farid, 'Finite element modeling of functionally graded piezoelectric harvesters', Composite Structures, 129 (2015) 165-176.

[27] S. C. Stanton, C. C. McGehee and P. Mann, 'Reversible hysteresis for broadband magnetopiezoelectric energy harvesting', Applied physics letters, 95 (2009) 1-3.

[28] S. Zhou, J. Cao, A. Erturk, and J. Lin, 'Enhanced broadband piezoelectric energy harvesting using rotatable magnets', Applied Physics Letters, 102, 173901 (2013).

[29] D. S. Ibrahim, A. G. A. Muthalif, T. Saleh, 'Piezoelectric based vibration energy harvester with tip attraction magnetic force: Modelling and simulation', Mathematics and Computers in Science and Industry, 23 (2014) 80-86.

[30] K. Q. Fan, F. B. Chao, J. G. Zhang, W. D. Wang and X. H. Che, 'Design and experimental verification of a bi-directional nonlinear piezoelectric energy harvester', Energy Conversion and Management, 86 (2014) 561–567.

[31] P. Kim and J. Seak, 'A multi-stable energy harvester: Dynamic modelling and bifurcation analysis', Journal of Sound and Vibration, 333 (2014) 5525–5547.

[32] J. Jung, P. Kim, J. I. Lee and J. Seok, 'Nonlinear dynamic and energetic characteristics of piezoelectric energy harvester with two rotatable external magnets', International Journal of Mechanical Sciences, 92 (2015) 206–222.

[33] M. W. Shafer and E. Garcia, 'The power and efficiency limits of piezoelectric energy harvesting', Journal vibration and Acoustics, 136 (2014).

[34] G. Litak, M. I. Friwell and S. Adhikari, 'Magnetopiezoelectric energy harvesting driven by random excitation', Applied Physics Letters, 96 (2010).

[35] S. Priya and D. J. Inman, 'Energy harvesting technologies' New York: Spring 2009.

APPENDIX- 1

FAST FOURIER TRANSFORMS WITH MATLAB

The functions $Y= fft(x)$ and $y=ifft(X)$ implement the transform pair given for vectors of the length N by following equations.

$$X(k)=\sum_{j=1}^{N} x(j)\times\omega_N^{(j-1)(k-1)} \tag{A.1}$$

$$x(j)=\left(1/N\right)\sum_{k=1}^{N} X(k)\times\omega_N^{-(j-1)(k-1)} \tag{A.2}$$

Here ω_N is an N^{th} root of unity and given by following equation.

$$\omega_N=e^{(-2\pi i)/N} \tag{A.3}$$

Solution technique:-

$Y= fft(x)$ returns the discrete Fourier transform (DFT) of vector x, computed with the fast Fourier transform algorithm. If the input X is matrix, $Y= fft(X)$ returns the Fourier transform of each column of the matrix. If the input X is multidimensional array, fft operates on the first nonsingleton dimension. $Y= fft(X,n)$ returns the n-point DFT. $fft(X)$ is equivalent to $fft(X,n)$, where n is the size of the X in the first nonsingleton dimension. $Y=fft(X,[\ ],dim)$ and $Y=fft(X,n,dim)$ applies the FFT operation across the dimension dim.

APPENDIX- 2

RUNGE-KUTTA SOLVER

It solves ordinary differential equations. The general steps for solving the equation $y'=f(x)$ with $y(0)=y_0$ are summarized in the following equations.

$$k\_1=hF\_xy\left[x(i),y(i)\right] \tag{A.4}$$

$$k\_2=hF\_xy\left[x(i)+0.5h,\left(y(i)+0.5\times h\times k\_1\right)\right] \tag{A.5}$$

$$k\_3=hF\_xy\left[x(i)+0.5h,\left(y(i)+0.5\times h\times k\_2\right)\right] \tag{A.6}$$

$$k\_4=hF\_xy\left[x(i)+h,\left(y(i)+k\_3\times h\right)\right] \tag{A.7}$$

$$y(i+1)=y(i)+\left(1/6\right)\times\left(k\_1+2\times k\_2+2\times k\_3+k\_4\right) \tag{A.8}$$

In the above equations, h is the step size. By using the main equation (A.8) and following the steps (A.4) to (A.7) Runge-Kutta solver solves the ordinary differential equation. The approach can be extended for second-order differential equations, where it is written as two first order differential equations. Matlab employs the ode45 function to solve ODE provided the function or functions are defined properly. We employed the ode45 for solving the equations in generation of time histories in this work.